Impact of *Plasmodium falciparum* patient-derived isolates on brain endothelium *in vitro*

Caroline Askonas[1*], Janet Storm[2*], Grazia Camarda[2], Alister Craig[2#] and Arnab Pain[1#]

[1] Pathogen Genomics Laboratory, Bioscience Program, Biological and Environmental Sciences and Engineering (BESE), Division, King Abdullah University of Science and Technology, Thuwal, KSA

[2] Tropical Disease Biology, Liverpool School of Tropical Medicine, Pembroke Place, Liverpool L3 5QA, UK

[#] Address correspondence to: alister.craig@lstmed.ac.uk , arnab.pain@kaust.edu.sa

[*]Authors contributed equally to this work. CA and JS determined CA would be listed first as they are an early career scientist and JS is already an established researcher.

Abstract

A hallmark of cerebral malaria is sequestration of *Plasmodium falciparum* infected erythrocytes (IE) within the brain microvasculature. Binding of IE to endothelium reduces microvascular flow and combined with an inflammatory response perturbs endothelial barrier function, resulting in breakdown of the blood-brain barrier (BBB). Furthermore, cytoadherence leads to activation of the endothelium and alters a range of cell processes affecting signalling pathways, receptor expression, coagulation, and disruption of BBB integrity. Here, we investigated whether cerebral malaria (CM) derived parasites elicit differential effects on human brain microvascular endothelial cells (HBMECs), as compared to uncomplicated malaria (UM) derived parasites. Patient-derived IE from UM and CM clinical cases, as well as non-binding skeleton-binding protein 1 knockout parasites, were overlaid onto TNF-activated HBMECs in a co-culture system. Gene expression analysis of endothelial responses was performed using Fluidigm probe-based assays of a panel of genes involved in inflammation, apoptosis, endothelial barrier function, and the prostacyclin synthesis pathway. We observed a significant effect on the endothelial transcriptional response in the presence of IE, yet there was no significant correlation between HBMEC responses and the type of clinical syndrome (UM or CM). Further, there was no correlation between HBMEC gene expression and both binding itself and the level of IE binding to HBMEC, as we detected the same change in endothelial responses when employing both binding and non-binding parasites. Our results suggest that interaction of IE with endothelial cells in this co-culture model induce some endothelial responses that are independent of clinical origin and independent of the expression of the major variant antigen *Pf*EMP1 on the IE surface.

Keywords: cerebral malaria, cytoadherence, Plasmodium falciparum, HBMEC, endothelium, gene expression

Introduction

In spite of global efforts to reduce mortality and morbidity of malaria, an estimated 249 million cases and 608,000 deaths were reported in 2022, with the majority occurring in children under the age of five [1]. The vast majority of infections result in mild febrile cases of uncomplicated malaria (UM), as severe disease only occurs in 1-2% of all cases [2]. Out of the eight *Plasmodium spp* that have been reported to cause either direct or zoonotic infection in humans, *P. falciparum* is considered a major driver of severe disease and mortality [3,4] . Cerebral malaria (CM) is a severe neurological complication of malaria infection that is a major cause of death, with mortality estimated between 15-25% and clinical manifestations including unarousable coma and seizures [5,6]. Mortality in paediatric CM is associated with brain swelling, which is considered to occur as a result of increased permeability of the blood-brain barrier (BBB) due to loss of

62 BBB function, leading to vasogenic oedema [6,7]. Continued study of the pathophysiology of CM is required
63 in order to develop targeted treatment therapies.
64
65 It is evident that CM is a complex, multi-component disease requiring a multifactorial view of pathogenesis
66 that considers the observed heterogeneous clinical manifestations of CM [8,9]. The sequestration of *P.*
67 *falciparum*-infected erythrocytes (IE) to brain microvasculature is a hallmark of CM. Cytoadhesion of IE
68 to the endothelium is mediated by *Plasmodium falciparum* erythrocyte membrane protein 1 (PfEMP1), a
69 variable surface protein that is expressed by IE and contains an extracellular binding region [10]. This highly
70 polymorphic protein is encoded by a group of approximately 60 *var* genes per parasite with monoallelic
71 expression, and the composition of the extracellular region confers binding to various host receptors [11].
72 Several vascular surface proteins, in particular CD36, EPCR, and ICAM-1, may serve as IE adhesion
73 receptors, and the expression of these endothelial receptors varies between vascular locations and is
74 modulated in part by cytokines, such as TNF and IFN [9,10,12,13]. EPCR is associated with severe malaria, as
75 PfEMP1s containing EPCR binding domains have been linked to brain swelling in paediatric CM [14-17].
76 While ICAM-1 mediates cytoadhesion related to sequestration in the brain [13-15], its direct role in the
77 pathology of CM is less clear. However, research has demonstrated that a subset of EPCR-binding parasites
78 have the ability to bind ICAM-1and that expression of these dual binders have been associated with CM in
79 patients [15,18,19].This cytoadherence alters a range of endothelial cell processes and leads to the activation of
80 endothelium as well as reducing microvascular flow. Accumulation of IE causes vessel occlusion and
81 generates microenvironments where both parasite factors and soluble erythrocytic content can accumulate
82 after IE rupture at the end of the parasites' intraerythrocytic cycle [8,20]. Ultimately, the contributions of both
83 microvascular obstruction and endothelial dysfunction lead to the disruption and breakdown of the BBB
84 [5,8,9,17].
85
86 Although IE derived from malaria patients have exhibited different binding phenotypes, most studies
87 employ well characterized PfEMP1 laboratory strains to investigate cytoadherence and interaction of
88 different PfEMP1 variants to brain endothelial cells [19,21-24]. Separate investigations have highlighted the
89 divergent effect of both TNF stimulation and IE cytoadhesion on endothelial transcriptional responses and
90 the pathways they induce [23,25]. IE isolated from peripheral blood of UM and CM patients have been used to
91 study cytoadherence to human brain microvascular endothelial cells (HBMEC). It was found that IE
92 isolated from CM patients exhibit differential binding capacities to TNF-activated brain endothelium *in*
93 *vitro*, as they were associated with increased adhesion [26]. Further study employing patient derived isolates

is needed to elucidate the impact of parasite cytoadhesion on the brain microvasculature in association with different disease outcomes.

The aim of this study is to investigate whether CM derived IE elicit differential effects on HBMEC as compared to UM derived isolates. An *in vitro* co-culture model of cytoadherence was employed wherein patient-derived IE isolates were overlayed onto TNF-activated HBMEC and the relative gene expression of HBMEC after incubation with either RBC or IE for a panel of genes was assessed. A study utilizing two *P. falciparum* lab strains with different binding capacities to HBMEC found that different PfEMP1-expressing variants induced divergent endothelial transcriptional responses during cytoadherence [25]. Differentially expressed genes (DEGs) were identified in HBMEC in pathways involved in the pathology of severe malaria, such as inflammation, apoptosis, and barrier integrity. From this list of DEGs, a panel of genes was compiled for this study, and gene expression was investigated by qPCR using the Fluidigm DELTAgene assays system. First, the relative gene expression of HBMEC after exposure to control RBC or IE for combined UM and CM derived isolates was compared, followed by comparing the expression data between clinical type. We observed variation in endothelial transcriptional responses to individual patient-derived parasite isolates as compared to RBC, but these responses did not show a significant differential combined effect between the UM or CM derived isolates. It was assessed whether the HBMEC relative gene expression after co-culture was correlated with the binding avidity of the parasite isolates, but a significant relationship was not observed. Our data confirm that IE have a profound effect on endothelial transcription that is specific to the presence of the *P. falciparum* parasites in the erythrocyte. However, we did not observe effects that were associated with disease severity with the panel of genes used in this study.

Materials and Methods

Culture of Endothelial Cells

Primary HBMEC were obtained from Cell Systems, USA (ACBRI 376) and were cultured in Endothelial Cell Growth Medium 2 (EGM2) media (C-22111, Promocell) supplemented with 2% foetal calf serum (FCS), 5 ng/mL epidermal growth factor (EGF), 10 ng/mL basic fibroblast growth factor, 20 ng/mL Long R3 IGF-1, 0.5 ng/mL VEGF 165, 1 µg/mL ascorbic acid, 22.3 µg/mL heparin, and 0.2 µg/mL hydrocortisone from the supplement pack (C-39211, Promocell). In order for the endothelial cells to adhere to the surface, flasks were coated with attachment factor (10308363, Gibco). Cells were passaged using Accutase solution (A6964, Sigma Aldrich), following manufacturer instructions. Cells were cultured in a 5% CO2 incubator at 37°C.

127 **Culture of *P. falciparum* Parasites**

128 Patient-derived *P. falciparum* parasites were isolated from peripheral blood from paediatric malaria cases
129 recruited at the Queen Elizabeth Central Hospital, Blantyre, Malawi with ethical approval from the College
130 of Medicine, University of Malawi and LSTM, as described in Storm et al [26]. Four UM and four CM patient
131 isolates were selected based on their cytoadherence profile to HBMEC and human dermal microvascular
132 endothelial cells and their ability to establish as a continuous culture. After isolation from blood, limited IE
133 could be cryopreserved, especially for CM isolates, only a maximum of 150 µl IE could be frozen.
134 Establishing the isolates as a continuous culture, expanding the cultures to generate more stabilates, and
135 subsequently have 65 ml of culture volume at 2% HCT for the co-cultures requires a considerable amount
136 of time. Therefore, co-cultures were performed after at least 21 DIC. The total DIC for the patient-derived
137 parasite isolates for co-culture 1 and 2, respectively, were UM1: 24 and 43, UM2: 21 and 32, UM3: 31 and
138 42, UM4: 24 and 25, CM1: 29 and 29, CM2: 35 and 44, CM3: 49 and 59, and CM4: 29 and 41. The skeleton-
139 binding protein knockout (SBP1-KO) lab strain was obtained from A.G. Maier and cultured in the presence
140 of 4 nM WR99210 [27].

141

142 The IE were cultivated at 2% haematocrit in O+ human erythrocytes and grown at 37°C in 25cm^2 tissue
143 culture flasks (T25) filled with a gas mixture of 96% nitrogen, 3% carbon dioxide, and 1% oxygen. The
144 duration of parasite culturing was isolate dependent, as different lengths of continuous culture were required
145 to generate enough material to perform the experiments, ranging from 14-60 days in culture (DIC). IE were
146 maintained in complete RPMI 1640 medium with 11 mM glucose and 0.2% sodium bicarbonate (R-0883,
147 Sigma) supplemented with 5% human serum, 0.25% Albumax II (11021029, ThermoFisher Scientific), 30
148 mM of HEPES (15630122, Gibco), 2 mM L-glutamine (G-7513, Sigma), 25 ng/mL gentamicin sulphate
149 solution (G-1271, Sigma), and 0.11 mM hypoxanthine (H9636, Sigma) pH 7.4. Parasite growth was
150 monitored using Giemsa staining (1092040500, Merck), and IE were passaged to maintain 2-5%
151 parasitaemia. Mixed-staged cultures were synchronized for ring stages using a 5% D-sorbitol solution
152 (S3889, Sigma), and IE at trophozoite stage were used for the *in vitro* co-culture studies with HBMEC. EC
153 cultures, parasite lines, culture media, and washed RBCs were monitored for mycoplasma contamination
154 using MycoBlue™ Mycoplasma Detector (Vazyme, D101-02).

155

156 **Co-culture of HBMEC and IE**

157 HBMEC at passage 5-8 were cultured until 90% confluency in T25 flasks. One day prior to co-culture,
158 HBMEC were seeded in 12-well plates at a density of 50,000 cells/cm^2 (for 3.8 cm^2 wells, this is equivalent
159 to total of 190,000 cells) in the morning and stimulated overnight with 10 ng/mL TNF (PHC3015,

160 Invitrogen). The RBC control was prepared by culturing a 2% haematocrit suspension in RPMI medium
161 overnight. On the day of the co-culture, the supernatant was removed from the HBMEC and replaced with
162 EGM2 media without heparin and hydrocortisone (EGM2min media) 2 hours prior to co-culture. IE were
163 enriched for mature stages by layering onto a 0.7% gelatine solution and incubation at 37°C for 45-60
164 minutes and after enrichment, the haematocrit and parasitaemia were calculated and IE suspensions were
165 prepared to an average parasitaemia of 30% (parasitaemia ranged from 20-40%, depending on enrichment
166 properties of the isolates) at 1% haematocrit in EGM2min media.

167

168 The RBC control was also subjected to gelatine treatment and a suspension at 1% haematocrit in EGM2min
169 media was prepared. EGM2min medium was used to maintain healthy HBMEC and did not affect parasite
170 viability in the 6-hour co-culture, but parasite development seemed delayed, as assessed by microscopy.
171 Medium was removed from the HBMEC, and 700 µl IE or RBC suspension were overlayed onto HBMEC
172 for 6 hours in a 5% CO2 incubator at 37°C, as well as EGM2min medium as an additional control. 700 µL
173 of 30% parasitaemia at 1% haematocrit is equivalent to $2.1x10^7$ IE and addition of the IE suspension to
174 HBMEC is equivalent to a ratio of 110 IE/HBMEC. A 0-hour control with EGM2min medium was used to
175 compare with the 6-hour time points. Control samples were generated by overnight incubation of HBMEC
176 with either 10 ng/mL of TNF, or 1 ng/mL IL-1 beta (579402, BioLegend) and compared to EGM2min
177 medium.

178

179 At each time point, the co-culture medium was removed, and the HBMEC were washed once with
180 EGM2min medium to remove unbound IE or uninfected RBC. Cells were directly lysed in the well using
181 350 µL of lysing solution (1% 2-mercaptoethanol in Buffer RLT; RNeasy Mini Kit, 74106, Qiagen) by
182 pipetting over the well. The lysates were collected into a 1.5mL sterile tube, vortexed, and stored at -80°C
183 until RNA extraction. Two independent co-culture experiments were performed for each patient isolate and
184 SBP1-KO.

185

186 In parallel to the co-culture experiments, activation of HBMEC after overnight incubation with TNF was
187 assessed. One day prior to co-culture, HBMEC were plated onto 24-well plates at a density of 50,000
188 cells/cm^2. The HBMEC were incubated overnight with either media alone or media containing 10 ng/mL
189 of TNF. Cells were detached with Accutase, collected in PBS + 1% FBS and stained for ICAM-1 expression
190 on the endothelial cell surface using APC anti-human CD54 antibody (353111, Biolegend). Flow cytometry
191 analysis was performed and confirmed that ICAM-1 expression was upregulated following overnight
192 stimulation with TNF in each of the co-culture experiments.

193

194 **RNA Extraction and Quality Assessment**

195 Frozen HBMEC lysates were placed in a 37°C water bath until thawed and salts dissolved. Total RNA was
196 purified using the RNeasy Mini Kit (74106, Qiagen) following the manufacturer's instructions using steps
197 4 -10 of the "Purification of Total RNA from Animal Cells using Spin Technology" protocol. RNA was
198 eluted in 50 µL of RNase-free water.

199

200 The RNA concentration of each sample was quantified using a Qubit fluorometer and the RNA High
201 Sensitivity assays (Q32852, Invitrogen), following manufacturer instructions. The quality of the RNA
202 samples was assessed using an Agilent 2100 Bioanlayzer (RNA 6000 Nano Kit, 5067-1511, Agilent
203 technologies) following manufacturer instructions. The RIN for all samples was between 9.4-10, indicating
204 high quality RNA.

205

206 **Gene Expression Assays using the Fluidigm System and Calculations**

207 Gene expression qPCR assays were conducted on the extracted RNA for a panel of 49 genes that include
208 pathways pertaining to inflammation, apoptosis, endothelial barrier function, and prostacyclin synthesis
209 (listed in Supplementary Table 1). In short, cDNA was prepared with reverse transcription before pre-
210 amplification (13-cycles) and clean-up of the reactions using Exonuclease 1, following the manufacturer
211 protocols (100-6472 B1, PN 100-5875 C1) and reagents (Fluidigm,100-6297; Fluidigm, 100-5580; New
212 England Biolabs, M0293S; TEKnova, 10221). Real-time PCR data was collected using the Biomark HD
213 system with a 96.96 IFC chip using Fluidigm Delta-Gene Assays on the pre-amplified cDNA. The
214 manufacturing protocol was followed for use of the Biomark HD system (PN 100-9792 A1) using the
215 reagents specified for preparing samples (Biorad, 172-5211; Fluidigm, 100-7609)) and assays (Fluidigm
216 100-7611; TEKnova, 10221). Technical replicates were performed for each sample, and Ct values were
217 obtained as the throughput of the real-time data. The primers for the gene panel were proprietarily designed,
218 prepared, and tested by Fluidigm.

219

220 Relative gene expression was calculated using the $2^{-\Delta\Delta Ct}$ method as previously described [28] using GAPDH
221 as the endogenous control (ΔCt) and the 6-hour EGM2min media-only sample as the normalization controls
222 (ΔΔCt). In this way, the exponential fold changes (FCs, $2^{-\Delta\Delta Ct}$) in the target genes are calculated as
223 normalized to the GAPDH internal control and relative to the expression of the HBMEC-media only at the
224 6-hour time point. For each target gene, the gene expression of HBMEC incubated with EGM2min media

225 at 6-hours is equal to 1 (baseline). Therefore, an FC>1 indicates increased relative gene expression and an
226 FC <1 indicates decreased relative gene expression for the experimental samples. FCs were calculated for
227 each technical triplicate of each sample for each experiment. To compare relative gene expression of
228 HBMEC after incubation with various groups (e.g., RBCs, UM parasite isolates, CM parasites isolates, or
229 combined IE), the mean, standard error of the mean (SEM), and confidence intervals for each group were
230 calculated from the technical triplicates of each sample for each independent experiment. Either two-tailed,
231 unpaired T-tests or Welch's T-test were then performed to compare the relative gene expression between
232 various corresponding groups. Additionally, a paired analysis was performed wherein the HBMEC-IE
233 relative gene expression for each parasite isolate was compared to the corresponding HBMEC-RBC relative
234 gene expression, for both experiments. For this analysis, the target FCs were calculated as normalized to
235 GAPDH and relative to the corresponding experimental 6-hour EGM2min media, and the mean and SD
236 were determined from the technical triplicates for each sample.

237

238 **Binding of Parasite Isolates to HBMEC under Flow Conditions**

239 The binding assay was performed using the Cellix microfluidics system as previously described [26,29].
240 Briefly, HBMEC were stimulated overnight with 10 ng/ml TNF, detached, and seeded in attachment factor
241 coated Vena8 biochips (Cellix). When cells formed a confluent monolayer, an IE suspension of 2%
242 parasitaemia and 5% haematocrit in binding buffer (RPMI 1640 with 25 mM HEPES, 11 mM glucose, 2
243 mM glutamine, pH 7.2) was flowed through for 5 minutes at 37 °C at a shear stress of 0.4 dyne/cm2. After
244 a washing step, bound IE were counted by microscopy in 15 areas throughout the biochip and the mean
245 IE/mm^2 EC cell surface calculated.

246

247 **Statistical Analysis**

248 Statistical analyses were performed on Prism 9 (Version 9.5.1, GraphPad Software). The exact statistical
249 tests, along with the levels of significance, are detailed in the figure legends.

250

251 **Data Availability**

252 Data will be made publicly available upon publication.

253

254

255

Results

Expression of intermediates involved in maintaining vascular barrier integrity is increased in HBMEC in response to patient-derived *P. falciparum* parasites.

To investigate endothelial responses to the patient-derived parasite isolates, we first compared the relative gene expression of TNF-activated HBMEC after six-hour exposure to either RBC or IE derived from patients with clinically defined UM or CM. Additional media-only samples were collected to be used as normalization controls in the relative gene expression calculations.

The relative gene expression of 49 target genes was analysed by grouping HBMEC samples by clinical type of the patient isolates, either HBMEC-UM or HBMEC-CM, and comparing them to the corresponding HBMEC-RBC control. Gene expression was calculated for HBMEC-UM, HBMEC-CM, and corresponding HBMEC-RBC by determining the mean FC±SEMs for each group relative to the corresponding 6-hour EGM2min media controls in each of the two independent experiments. Welch's t-tests were performed to compare the relative gene expression of the HBMEC-IEs to their corresponding HBMEC-RBC controls, and the mean FC±SEMs are reported in Supplementary Table 1, along with the Welch's t-test results.

Differential gene expression was observed in HBMEC in the presence of IE compared to the corresponding RBC control for a number of genes, and several were selected for further study due to their relatively increased expression (FC > 1.7), as well as the biological processes they are involved in. These genes encode: B-cell lymphoma 2-related protein A1 (*BCL2A1*), cytochrome P450 family 1 subfamily A member 1(*CYP1A1*), Krüppel-like factor 2 (*KLF2*), Krüppel-like factor 4 (*KLF4*), prostacyclin synthase (*PTGIS*), and prostaglandin-endoperoxide synthase 2, also known as cyclooxygenase-2 or Cox-2 (*PTGS2*).

Maintenance of the blood-brain barrier is achieved by balancing inflammation, apoptosis, and repair, among other processes, at the microvascular endothelial cell surface [9,30]. *BCL2A1* is a member of the pro-survival sub-family of BCL2 proteins that include both pro- and anti-apoptotic regulators, and it encodes a protein that reduces the release of pro-apoptotic cytochrome C and blocks caspase activation [31,32]. Expression of *BCL2A1* is upregulated in vascular endothelial cells by the inflammatory cytokines TNF and IL-1beta [33,34]. Furthermore, it has been observed that monocytes induce expression of *BCL2A1* and confer protection against apoptosis after direct cell-cell contact [33]. Several Krüppel-like transcription factors have diverse functions that indicate them as key regulators of endothelial biology. Both *KLF2* and *KLF4* are implicated

288 in maintaining vascular and endothelial integrity, and their expression is modulated by both changes in
289 laminar sheer flow or stress and pro-inflammatory stimuli [35,36]. In *in vitro* studies, KLF4 was shown to
290 inhibit expression of inflammatory mediators VCAM-1 and tissue factor (TF) while enhancing expression
291 of endothelial nitric oxide synthase (eNOS) and thrombomodulin (TM) [37,38]. In a similar manner, KLF2
292 induces eNOS and TM expression and activity, and inhibits both IL-1beta and NF-kappaB mediated
293 induction of adhesion molecules, such as VCAM-1 and E-selectin, and adhesion of immune cells [39,40].
294 Furthermore, overexpression of KLF2 inhibited TNF-mediated induction of TF and plasminogen activator
295 inhibitor-1 (PAI-1) [40].

296

297 CYP1A1, PTGIS, and PTGS2 are involved in eicosanoid, prostanoid, and prostacyclin biosynthetic
298 pathways, which produce various lipid mediators that regulate inflammatory responses (Figure 1) [41].
299 CYP1A1 is a member of the cytochrome P450 enzyme family that metabolizes a range of substrates,
300 including arachidonic acid [42]. Both PTGIS and PTGS2 are enzymes involved in the biosynthesis of
301 prostacyclin, a bioactive lipid that is produced by vascular endothelial cells and that plays a role in
302 regulation of endothelial inflammation and apoptosis [41]. Furthermore, a study employing a co-culture model
303 of cytoadherence demonstrated differential gene expression of *CYP1A1*, *PTGIS*, and *PTGS2* between
304 HBMEC incubated with two parasite lines that expressed different *Pf*EMP1s [25].

305

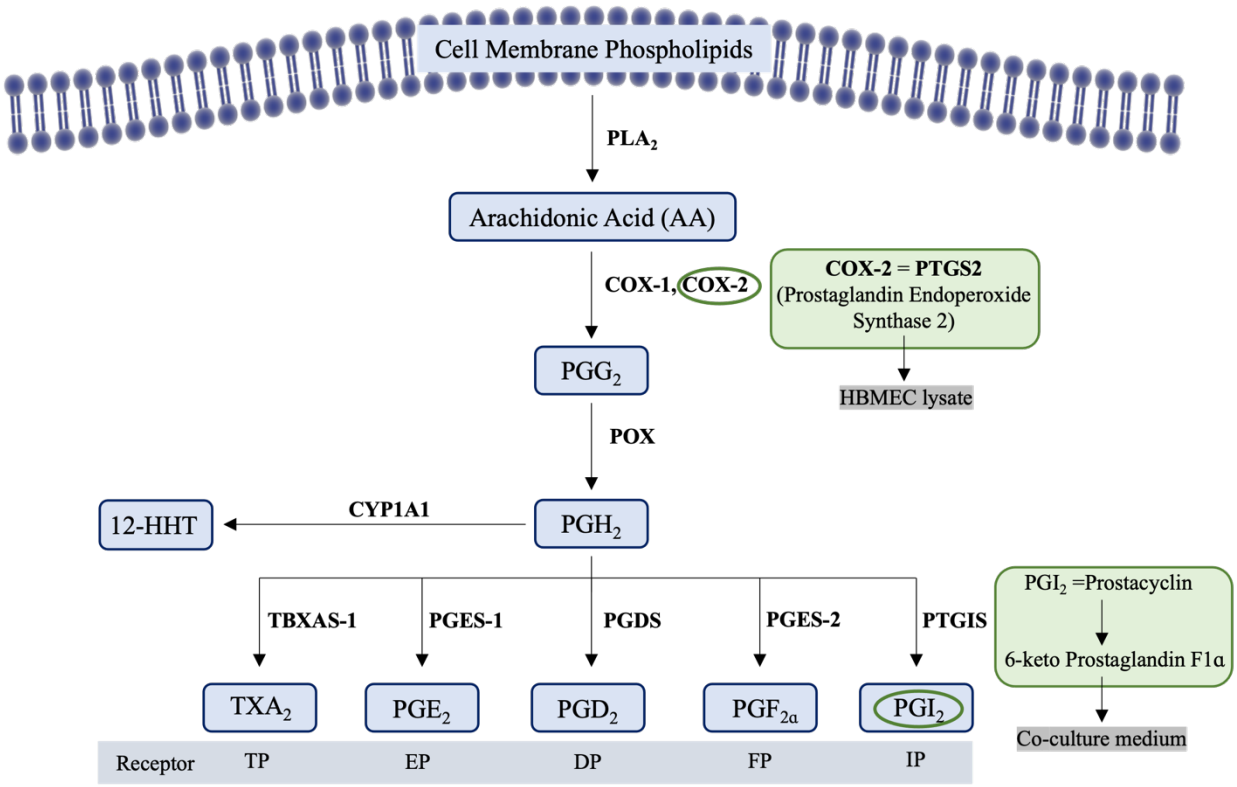

Figure 1: **The biosynthetic cascade of prostacyclin and other prostanoids.** Arachidonic Acid (AA) is hydrolysed from membrane phospholipids by phospholipase A2 (PLA_2), which is then metabolized by cyclooxygenase (COX) enzymes to form the precursor prostaglandin G_2 (PGG_2). This intermediate is modified by a peroxidase enzyme (POX) to form prostaglandin H_2 (PGH_2), which is further metabolized by specific synthase enzymes to yield various prostaglandins and thromboxane A_2 (TXA_2). Prostacyclin (PGI_2) is produced through the action of prostacyclin synthase (PTGIS; also known as prostaglandin I_2 synthase, PGIS). PTGS2 (COX-2) and PGI_2's hydrolysis product, 6-keto prostaglandin F1α, were detected in HBMEC lysate and co-culture medium, respectively. Adapted from Stitham et al. [41]

A significant increase in expression of *BL2A1*, *CYP1A1*, *KLF2*, *KLF4*, *PTGIS*, and *PTGS2* was observed for HBMEC after co-culture with both clinical isolate types as compared to the RBC controls (Figure 2, Supplementary Table 1). The mean HBMEC gene expression after co-culture was compared in two ways: grouping by clinical syndrome compared to the corresponding RBC and grouping by combining all IE samples compared to the corresponding RBC. The results of the Welch's t-tests for each gene are shown in Figure 2, with a sub-figure for each showing the combined data for HBMEC-RBC and HBMEC-IE co-culture, with paired data points from the same experiment joined by a line. This allows visual verification of increased gene expression within each experiment, which corresponds to the increase in gene expression observed when samples are grouped by clinical type. A paired t-test was performed comparing the mean FC of the HBMEC-RBC controls to the grouped HBMEC-IE for all the genes. There was a significant increase in expression of these genes by HBMEC in response to exposure to IE.

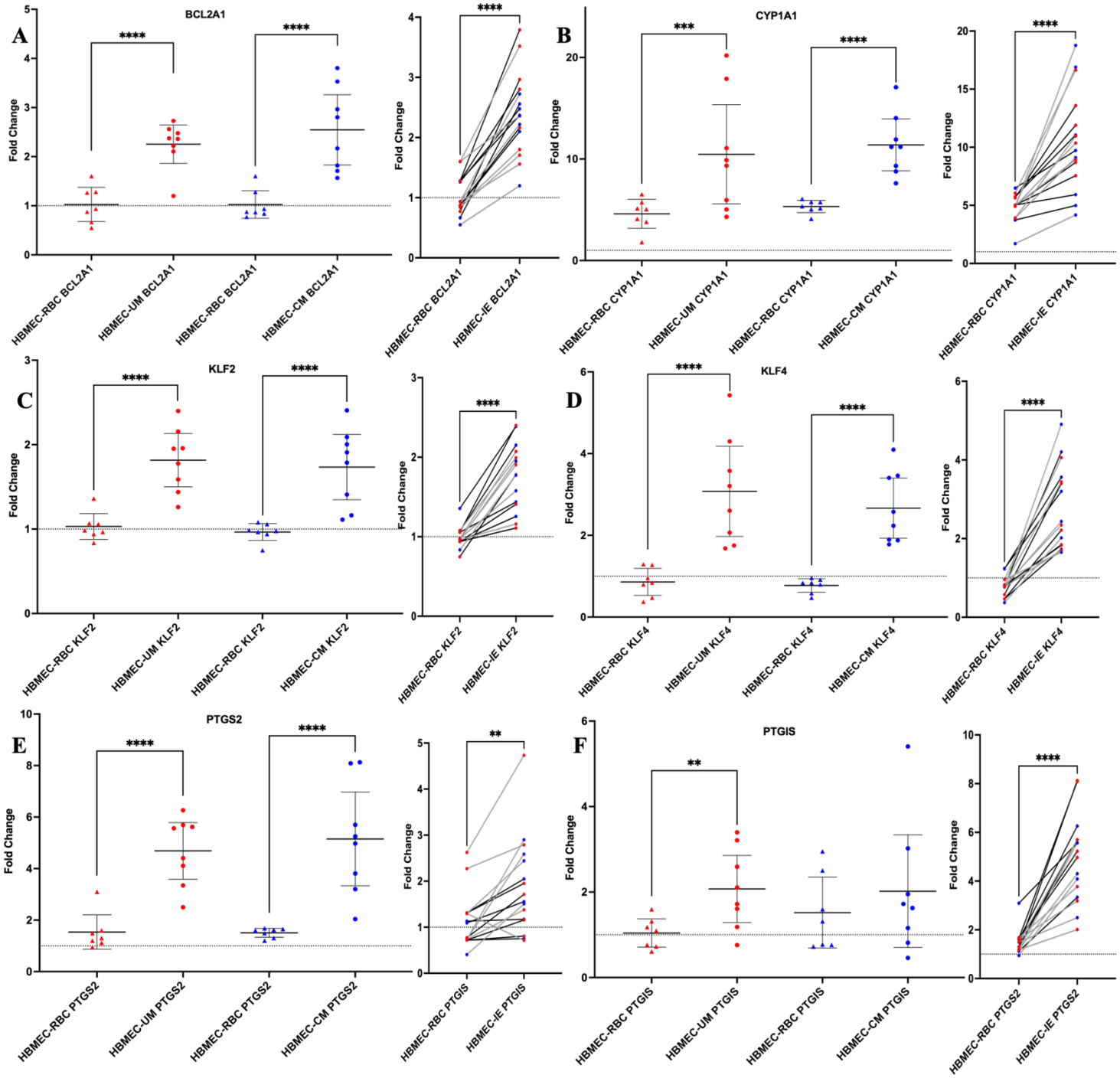

Figure 2: **IE of both UM and CM clinical isolates affect HBMEC transcriptional responses as compared to RBC**. Differential gene expression of HBMEC after 6-hour co-culture with patient-derived parasites compared to their corresponding RBCs for *BCL2A1*(A), *CYP1A1*(B), *KLF2*(C), *KLF4*(D), *PTGIS*(E), and *PTGS2*(F), calculated as relative to the corresponding 6-hour HBMEC-media control. Mean HBMEC gene expression (Fold Change) was compared in two ways for the selected genes: (left) Welch's t-test comparing HBMEC-RBC and HBMEC-IE for UM or CM isolates and (right) paired t-test comparing all RBC controls and the combined HBMEC-IE of all isolates. The Welch's t-test results shown in the graphs are from Supplementary Figure1. Each point on the plot represents one sample FC, calculated as a mean of the technical triplicates, and the mean and 95% confidence intervals are indicated for each group. For the paired analysis, the mean FC was calculated from technical triplicates

for each IE and corresponding RBC sample and are coloured red for UM isolates and blue for CM isolates. A paired t-test was performed comparing the mean FC of HBMEC-IE with the corresponding HBMEC-RBC. Lines between the groups indicate that the RBC sample on the left was the control for the corresponding isolate sample on the right. Black lines represent samples from experiment 1, and grey lines represent samples from experiment 2. Two-tailed tests were performed for both analyses, and the dotted line in the plots marks the baseline of FC=1. Significance is depicted by the P-value: *,0.01-0.05; **, 0.001-0.01; ***, 0.0001-0.001; ****, <0.0001.

To validate the observed changes in gene expression, we tested whether this co-culture model and the Fluidigm panel would reflect gene upregulation by incubating HBMEC with IL-1beta and TNF overnight and comparing the relative gene expression of the stimulated HBMEC with a media control (Table 1). Indeed, incubation with these stimuli resulted in upregulation of expression in HBMEC in the majority of tested genes, with notably large fold changes observed in both treatment groups for the following (IL-1beta and TNF, respectively): *CXCL3* (1305 and 862), *ICAM1* (16 and 25), *PTGS2* (30 and 16), *SELE* (1305 and 862), and *VCAM1* (548 and 873).

Table 1: **Validation of the co-culture model and Fluidigm panel through relative gene expression of HBMEC after overnight incubation with inflammatory cytokines**. HBMEC were incubated overnight with either EGM2min media, 1 ng/mL IL-1beta, or 10 ng/mL TNF, and the relative gene expression was determined for several genes. FCs were calculated using GAPDH as an endogenous control as relative to the HBMEC-overnight media normalization control (baseline is FC=1). The mean FC for each gene was calculated from technical triplicates from one experiment (n=3).

GENE	HBMEC-OVN MEDIA RELATIVE FC	HBMEC OVN IL-1B RELATIVE FC	HBMEC-OVN TNF RELATIVE FC
BCLA2A1	1	4.7	6.0
CXCL3	1	1305	862
CYP1A1	1	1.1	0.6
ICAM1	1	16	25
IL1A	1	40	30
IL1B	1	60	5.4
KLF2	1	1.1	1.0
KLF4	1	3.1	2.9
PTGIS	1	0.8	1.2
PTGS2	1	30	16
SELE	1	72	52
VCAM1	1	548	873

As previous studies have demonstrated that TNF differentially regulates transcriptional effects on brain endothelial cells [23,43], such as upregulated expression of *BCL2A1* in vascular endothelial cells [34], 0-hour data was collected to assess if the observed HBMEC FC expression was either due to activation with TNF or was due to effect of IE. In order to demonstrate the impact of TNF withdrawal, the relative gene expression of activated HBMEC after 2-hours (0-hour timepoint) and 8-hours (6-hour timepoint) incubation with media were compared for representative samples (Figure 3). There was significant reduction of relative FC levels of KLF4, PTGS2, ICAM-1, VCAM-1, and an observed reduction in BCL2A1 in HBMEC after withdrawal of TNF after 8 hours. Overall, these findings show that the differences in relative gene expression observed after co-culture are not artifacts of overnight TNF stimulation of the HBMEC.

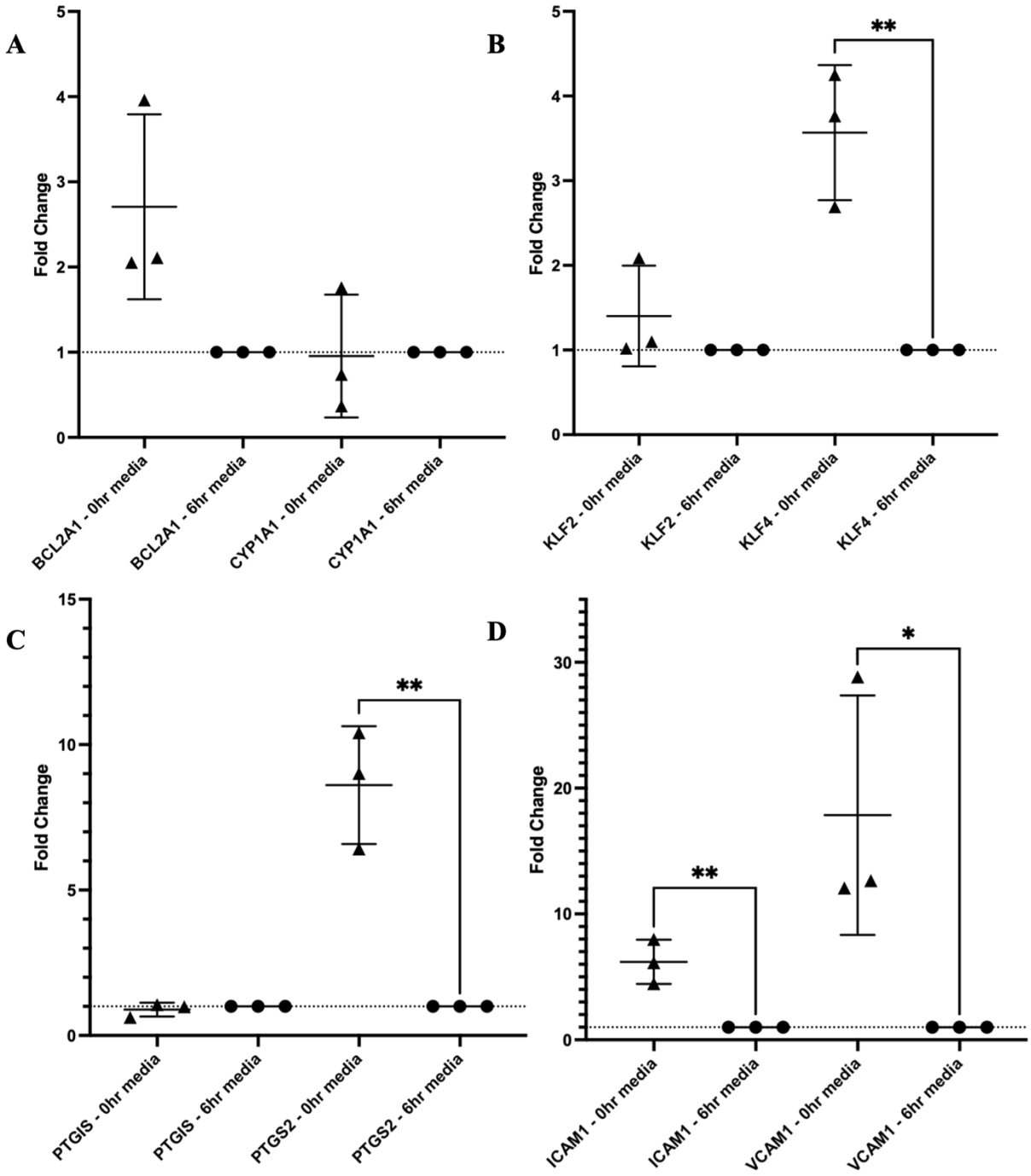

Figure 3: **Representative relative gene expression of HBMEC after withdrawal of TNF stimulation.** In the co-culture model, HBMEC are stimulated overnight with 10 ng/mL of TNF to stimulate the cells. The next morning, the supernatant containing TNF was removed and replaced with EGM2min media for two hours before co-culture experiments commenced. HBMEC-media samples were collected at 0hr and 6hour culture time points, corresponding to 2- and 8-hours incubation with EGM2min media and without TNF, respectively. Relative gene expression was determined for (A) *BCL2A1* and *CYP1A1*, (B) *KLF2* and *KLF4*, (C) *PTGIS* and *PTGS2*, and (D) *ICAM-1* and *VCAM1* for HBMEC-media samples for three independent, representative experiments (n=3). FCs were calculated using GAPDH as an endogenous control as relative to the HBMEC-6hour media normalization control (baseline is FC=1). Each plot point represents a mean of the technical triplicates, and the mean ± SD of the 3 experiments is shown with triangle points representing HBMEC-0hr media samples and circular points representing HBMEC-6hr media samples.

376
377 ***P. falciparum* parasites derived from uncomplicated or cerebral malaria cases do not induce divergent**
378 **HBMEC responses for the genes tested.**

379 To determine whether the observed effect on HBMEC responses to RBCs infected with the patient-derived
380 parasite isolates was specific to the clinical syndrome, the effect of RBCs on HBMEC was normalized. In
381 order to take into account variation in the RBCs for each experiment, gene expression FCs ($2^{-\Delta\Delta Ct}$) were
382 calculated relative to the corresponding 6-hour HBMEC-RBC sample, which was used as the normalization
383 control (ΔΔCt). Mean gene FCs were calculated for each clinical isolate type, grouped as HBMEC-UM and
384 HBMEC-CM, using the triplicates of all the experimental samples. Unpaired t-tests were performed to
385 compare the mean relative gene expression of the HBMEC-UM to the HBMEC-CM co-cultures (Figure 4).
386 With the exception of *PTGIS*, there was no differential effect of type of clinical isolate on HBMEC
387 transcriptional responses when comparing UM and CM patient-derived isolates.

388

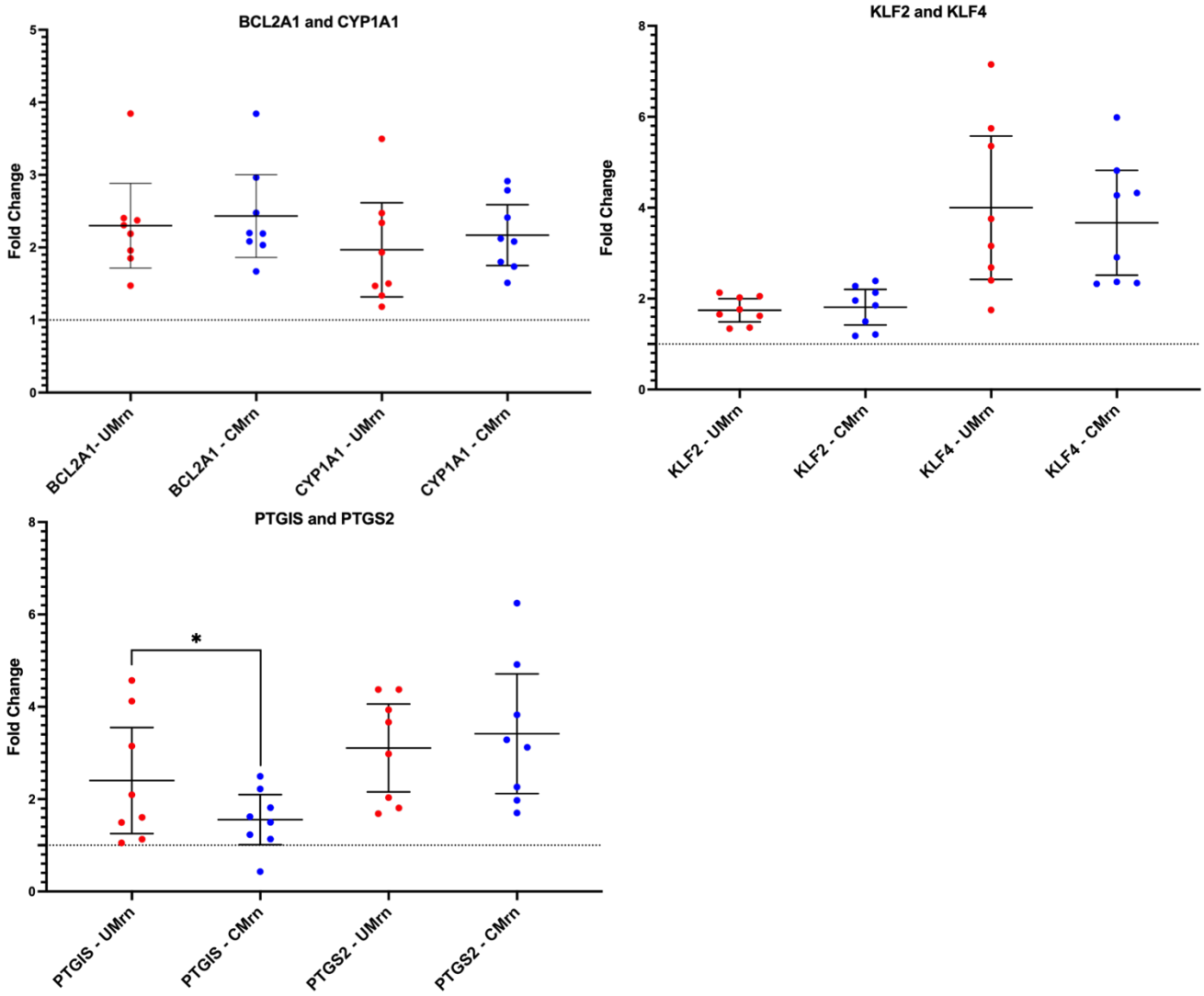

Figure 4: **Isolates within clinical categories do not induce differential responses in HBMEC.** To determine the effect of the parasites, HBMEC relative gene expression when exposed to UM and CM isolates was calculated relative to HBMEC-RBC expression, using GAPDH as the endogenous control and the 6-hour HBMEC-RBC as the normalization sample reference. Each point represents one experimental sample (mean of triplicates), and the mean FC and 95% confidence intervals for each gene was calculated using both biological replicates (n= 8). RBC normalized HBMEC-UM is represented as "UMrn", and RBC-normalized HBMEC-CM is represented as "CMrn". Significance between the two clinical categories was determined by two-tailed unpaired T-tests with P-value summary defined =*,0.01-0.05. The dotted line marks the baseline of FC=1 (red = UM isolates; blue = CM isolates).

The isolates chosen for this study were from a panel of patient-derived *P. falciparum* parasites, isolated from paediatric uncomplicated and cerebral malaria cases recruited at the Queen Elizabeth Central Hospital, Blantyre, Malawi as described in Storm et al [26]. The initial selection of the four UM and four CM patient isolates was based on their different cytoadherence to HBMEC and human dermal microvascular endothelial cells profiles after isolation from peripheral blood, as well as their ability to be established under *in vitro* culture conditions. During extended periods of culture, as well as when establishing *in vitro P.*

405 *falciparum* culture lines from patient parasite isolates, the *var* gene transcription profiles may change
406 dramatically, which could affect phenotypic changes, such as binding to HBMEC [44,45]. To establish the
407 isolates in culture and expand the volume to sufficient levels, the experiments were carried out after
408 culturing the IE for 14-60 days. To determine if their adherence to HBMEC had changed due to var gene
409 switching over time [44,45], binding assays under flow conditions were performed as close to the length of
410 culture time (days in culture, DIC) as the DIC for each co-culture experiment (Figure 5). Compared to their
411 initial binding phenotype, all isolates showed altered binding to HBMEC. UM1, UM3, UM4, CM2 and
412 CM3 increased their binding after various days in culture, with some variation between the two sets of DIC,
413 and UM2 and CM4 decreased their binding. The SBP1-KO strain does not bind to HBMECs.

414

415 Using data from both experiments, the binding capacities of the isolates were then correlated with the mean
416 gene expression (FC calculated using the 6-hour RBC as the normalization control) of HBMEC following
417 co-culture with IE using Spearman's correlation. These calculations were performed for the entire gene
418 panel by grouping the data per experiment, and representative plots for *KLF4*, *PTGIS*, and *PTGS2* are
419 presented in Supplementary Figures 1A and 1B for experiment 1 and experiment 2, respectively. After co-
420 culture, there was no observed significant correlation between the binding avidity of the parasites and the
421 HBMEC gene expression.

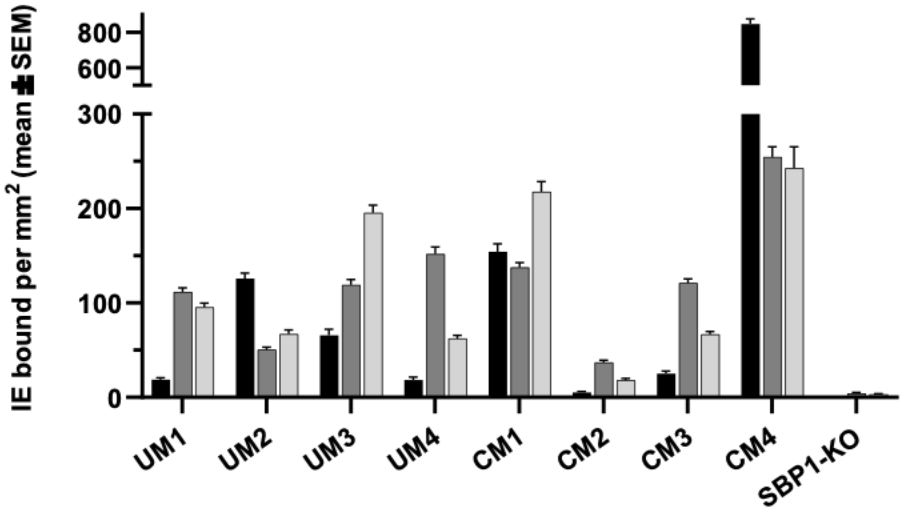

422

423 ***Figure 5:*** **Binding of patient isolates to HBMEC under flow conditions.** Binding of IE to TNF-stimulated HBMEC was
424 determined using microfluidics. Shown is the mean ± SEM IE/mm^2 EC cell surface of 15 fields counted by microscopy. The level
425 of binding for the UM and CM isolates at the time of isolation from the patients is depicted in black and after days in culture (DIC)
426 of 2 independent cultures in dark and light grey as follows; UM1: 64 and 30 DIC, UM2: 50 and 32 DIC, UM3: 44 and 40 DIC,
427 UM4: 38 and 25 DIC, CM1: 31 and 36 DIC, CM2: 46 and 32 DIC, CM3: 66 and 50 DIC, CM4: 46 and 42 DIC. SBP1-KO does
428 not bind to HBMEC.

429 **Observed differential effects of *P. falciparum* parasites on HBMEC responses is not solely due to**
430 **binding.**

431 To further investigate whether the observed differential effects on HBMEC transcriptional responses were
432 due to the direct interaction between the IE and the surface of HBMEC, two co-culture experiments were
433 performed using the non-binding parasite strain, skeleton-binding protein knockout parasites (SBP1-KO).
434 These parasites are unable to traffic *Pf*EMP1 to the infected erythrocyte surface, and therefore, they are
435 unable to bind to endothelium [27,46], verified by using flow binding assays to HBMEC (Figure 5). The relative
436 mean gene expression was calculated for the technical and biological replicates. Welch's t-tests were
437 performed to compare the relative FC of the HBMEC-SBP1KO parasites and the HBMEC-RBC controls
438 (Supplementary Table 2). The relative gene expression of the HBMEC incubated with the binding patient-
439 derived parasites (HBMEC-binding IE), and non-binding SBP1-KO parasites, as compared to the HBMEC-
440 RBC controls, are shown in Figure 6 for *BCL2A1*, *CYP1A1*, *KLF2*, *KLF4*, *PTGIS*, and *PTGS2*.

441

442 Even though similar effects were observed from the SBP1 knock-out parasites on HBMEC transcriptional
443 response when compared to the patient-derived isolates for these genes, the magnitude of the effect is not
444 always the same between HBMEC-SBP1-KO and the HBMEC-binding IE. The relative FC of the HBMEC-
445 binding parasites and the HBMEC-SBP1KO parasites were compared using Welch's t-tests (Supplementary
446 Table 3), and out of the genes presented in Figure 6, there were significant differences between the results
447 produced by binding and non-binding parasites for *BCL2A1*, *KLF4*, and *PTGS2*. Additionally, there is large
448 variation in responses within the binding-IE group, likely due to the expression of different
449 *Pf*EMP1variants. This suggests that more than one process is occurring, one of which is adhesion
450 independent. The observed differential effect on HBMEC transcriptional responses is related to parasite-
451 infected RBC, but not exclusively binding via *Pf*EMP1.

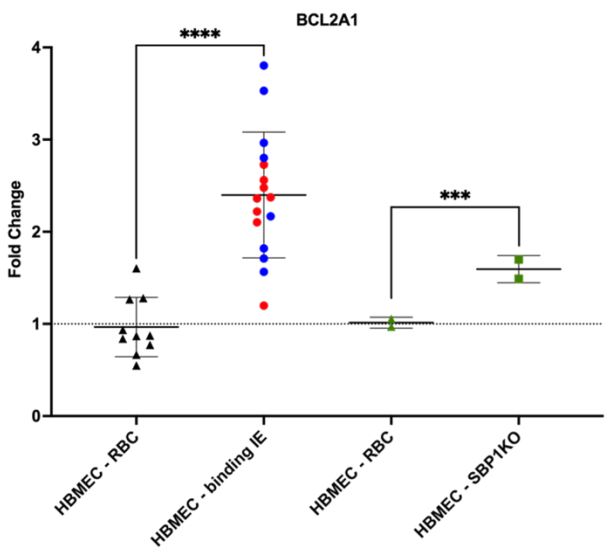
BCL2A1
****
***
Fold Change
0
1
2
3
4
HBMEC - RBC
HBMEC - binding IE
HBMEC - RBC
HBMEC - SBP1KO

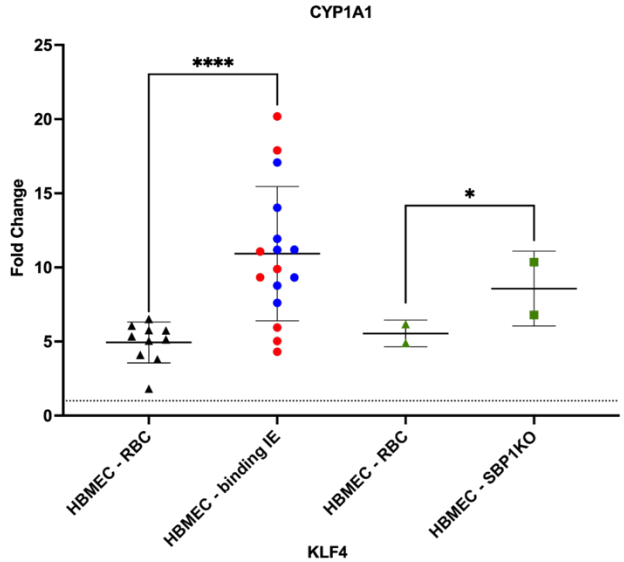
CYP1A1
****
*
Fold Change
0
5
10
15
20
25
HBMEC - RBC
HBMEC - binding IE
HBMEC - RBC
HBMEC - SBP1KO

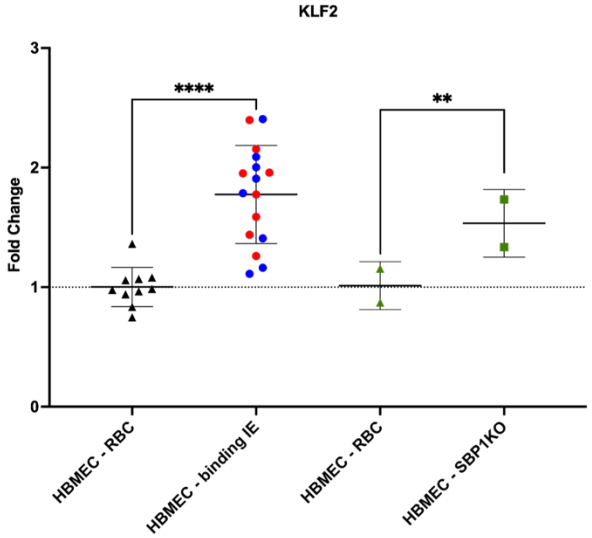
KLF2
****
**
Fold Change
0
1
2
3
HBMEC - RBC
HBMEC - binding IE
HBMEC - RBC
HBMEC - SBP1KO

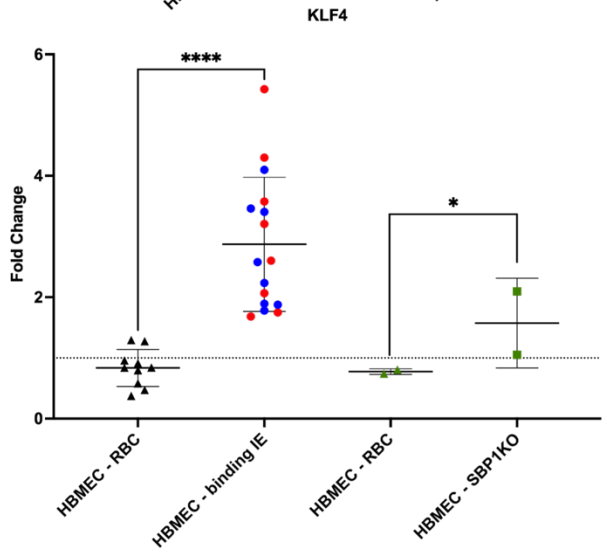
KLF4
****
*
Fold Change
0
2
4
6
HBMEC - RBC
HBMEC - binding IE
HBMEC - RBC
HBMEC - SBP1KO

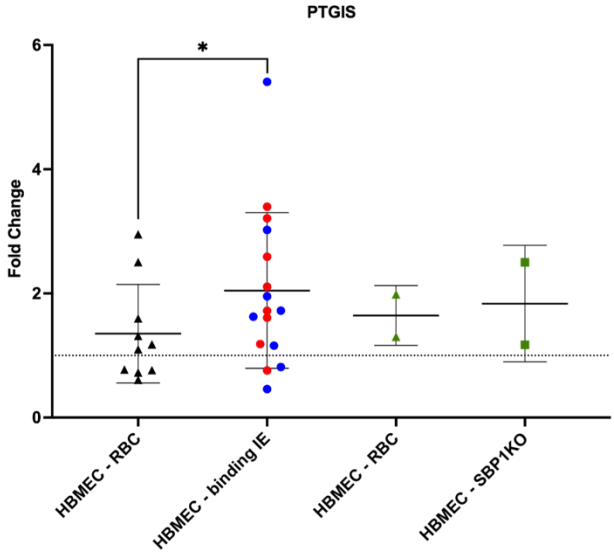
PTGIS
*
Fold Change
0
2
4
6
HBMEC - RBC
HBMEC - binding IE
HBMEC - RBC
HBMEC - SBP1KO

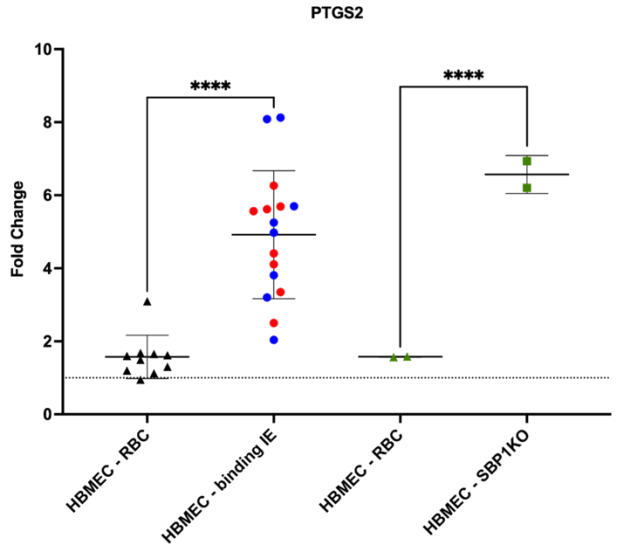
PTGS2
****
****
Fold Change
0
2
4
6
8
10
HBMEC - RBC
HBMEC - binding IE
HBMEC - RBC
HBMEC - SBP1KO

452

453 ***Figure 6:*** **Observed differential effects on HBMEC transcriptional response is not due to binding to HBMEC.** Relative gene
454 expression of HBMEC exposed to patient-derived parasites that bind to HBMEC and the non-binding SBP1-KO parasites for 6
455 hours compared to corresponding RBCs for select genes. FC was calculated using GAPDH as an endogenous control and relative
456 to the 6-hour HBMEC-media normalization control (baseline is FC =1). Welch's t-tests were used to compare HBMEC-RBC and
457 HBMEC-IE for each of the parasite groups, and the mean FC ± SEM for each gene was calculated using the two biological replicates
458 for 4 UM and 4 CM isolates and their corresponding RBC (HBMEC-RBC (binding) n = 10, HBMEC-binding IE n =16, HBMEC-
459 RBC(SBP1KO) and HBMEC-SBP1KO (n =2). The results of the Welch's t-tests are summarized in Supplementary Table 2. Sample
460 grouping is represented by symbol, with triangles for HBMEC-RBC, circles for HBMEC-binding IE, and squares for HBMEC-
461 SBP1KO. For binding IE, the red data points represent UM samples, while the blue data points represent CM samples. Samples
462 from experiments with the non-binding parasites are in green. Significant relationships are indicated by bars ($p<0.05$), and the
463 dotted line marks the baseline of FC=1. P-value summary defined= *,0.01-0.05; **, 0.001-0.01; ***, 0.0001-0.001; ****, <0.0001).
464 The P-value summaries are from the calculations performed in Supplementary Table 2.

465

466 As shown in Figure 5, differences in cytoadhesion of the patient isolates to HBMEC were measured after
467 culturing. To determine PfEMP1 domains expressed, *var* genotyping by qPCR was used and the data
468 compared to the qPCR data from when the parasites were isolated from the patients (Supplementary Table
469 4) [26]. As expected, some *var* gene switching has occurred, but UM4 and CM1 seemed to maintain similar
470 high transcripts for the same *var* domains.

471

472 **Determination of prostaglandin endoperoxide synthase 2 and prostacyclin production in HBMEC-**
473 **IE co-cultures**

474 HBMEC-IE co-culture activates the prostacyclin pathway as shown for *PTGIS* and *PTGS2* in the Fluidigm
475 results (Figure 2). Whether that results in increased concentrations of its end-product prostacyclin or the
476 intermediate prostaglandin endoperoxide synthase 2 (PTGS2) was determined by ELISA. Prostacyclin is
477 secreted but has a short half-life and therefore its hydrolysis product, 6-keto prostaglandin F1α (6-keto
478 PGF1α) was measured in co-culture medium of HBMEC-IE and compared with their respective HBMEC-
479 RBC controls (Supplementary Table 5). Overall, there is some variability between the experiments; co-
480 culture with UM3 produces significantly more 6-keto PGF1α than co-culture with RBC in only one of the
481 replicates in experiment 1, but not in experiment 7. Similarly for co-culture with UM2, a significant increase
482 of 6-keto PGF1α in seen in experiment 4, but not experiment 8, due to a large standard deviation. The ratio
483 6-keto PGF1α produced in HBMEC-IE compared to HBMEC-RBC varies from approximately 0.5 to 2,
484 with an outlier of 4.8 for HBMEC-UM2 (experiment 8) and there is no significant difference between
485 HBMEC-UM and HBMEC-CM after 6 hours co-culture (Supplementary Figure 2).

486

487 For the CM4 isolate and SBP1-KO, a co-culture of 20 hours was also performed (experiments 12 and 13),
488 and although more 6-keto PGF1α was produced, there was no significant increase compared with HBMEC-
489 RBC co-cultures. TNF stimulation of HBMEC does increase 6-keto PGF1α production approximately three
490 to six times and 15-minute treatment with thrombin results in a 10-fold increase in 6-keto PGF1α. The latter

491 is a known fast acting stimulator of prostacyclin production [47,48] and serves as a positive control for the
492 ELISA. PTGS2 was detected in HBMEC cell lysate after co-culture and calculated as ng PTGS2 per mg
493 total lysate protein (Supplementary Table 5). Overall, there was a small decrease in PTGS2 generation after
494 HBMEC-IE co-culture, but only significant for CM1 (experiment 9) and CM4 (experiment 6).

495

496 **Production of cytokines by HBMEC-IE co-cultures**

497 To determine if the production of cytokines or chemokines by HBMEC was altered following co-culture, a
498 multiplex panel of 41 secreted cytokines and chemokines was used. The multiplex was performed at an
499 early stage of the study and only included 6-hour co-culture medium of 3 CM isolates, 2 UM isolates and
500 two lab strains IT4var14 and IT4var37 in one experiment. These lab strains were included because they
501 were used in previous co-culture experiments [25]. Concentrations higher than 5 pg/ml were detected for 13
502 cytokines and only a few of these were significantly increased after co-culture with IE, compared to co-
503 culture with their respective RBC control (Supplementary Table 6). CM4, the isolate with the highest
504 binding to HBMEC, significantly increases production of IL-6, IL-8 and IP-10, as well as GRO, G-CSF
505 and GM-CSF. Although at low levels, IFNγ was increased two to ten-fold by co-culture with the patient
506 isolates, but not significantly by the lab strains IT4var14 and IT4var37. A positive control of TNF activated
507 HBMEC was included to produce high enough levels of cytokines to be measured, and for 10 analytes these
508 were at least 10-fold higher than medium only. Interestingly, after 16 hours TNF was still detectable at ~11
509 ng/ml in the culture medium.

510

511 **Effect of IE co-culture on HBMEC barrier integrity**

512 Although the cytoadherence phenotype of the isolates to HBMEC has been altered by time in culture, there
513 are still detectable differences, especially between CM2 and CM4 with low and high binding respectively.
514 Whether differential binding capacity of the patient isolates could affect HBMEC barrier function was
515 determined by real time trans endothelial electrical resistance (TEER). Barrier function increased slightly
516 by adding RBC, irrespective if they were infected or not (Supplementary Figure 3B) and no differences
517 between the patient isolates nor with different parasitaemia were detected. Thrombin induces a rapid
518 decrease in barrier function, which recovers within 2 hours and the presence of RBC and IE partly protected
519 against this effect by reducing the maximum decrease (Supplementary Figures 3C and 3E) and the rate of
520 recovery, determined by the area under the curve (AUC) (Supplementary Figures 3D and 3F). RBC and IE
521 all significantly reduced thrombin-induced decrease in barrier function compared to medium, but IE was
522 not significantly different to RBC. The recovery rate was more rapid with a significantly reduced AUC for
523 RBC, 5%, 10% and 30% IE compared to medium with a trend of more rapid recovery with increasing

524 parasitaemia. The AUC for SBP1-KO at the different parasitaemias were similar and not distinct compared
525 to medium, but all significantly different than the AUC of 30% IE, which had the smallest AUC at 13.5. No
526 differences between the individual UM and CM isolates could be detected.

527

528 **Discussion**

529 Cerebral malaria is a multifactorial disease that has been extensively investigated, although many questions
530 remain regarding its pathogenesis. A view of CM pathology has emerged in recent years that proposes
531 dysregulation of coagulation pathways, inflammation, release of parasite factors from mature IE, and the
532 sequestration of IE in the vasculature all contribute to endothelial dysfunction and, ultimately, the
533 breakdown of the BBB [8,9,49]. Cytoadhesion of IE to endothelial cells is one of the events in a multi-step
534 process leading to localized accumulation of both IE and RBC, and rupture and release of parasite and
535 intercellular erythrocyte components and soluble factors, resulting in activation of the endothelium and
536 immune responses, compromising BBB integrity [20,50]. Binding of *P. falciparum* IE to EPCR is correlated
537 with paediatric CM [15], and this cytoadhesion affects the thrombomodulin/EPCR axis, resulting in a decrease
538 in activated Protein C levels [51,52]. This modulation affects the integrity of the BBB and is one mechanism
539 whereby sequestration can have a devastating effect in the brain.

540

541 In the present study, HBMEC responses to clinically derived parasites isolates from UM and CM patients
542 were investigated by employing an *in vitro* co-culture model of cytoadhesion, wherein IE are overlayed
543 onto TNF-activated HBMEC for 6 hours and measuring relative gene expression of 49 genes by Fluidigm
544 Delta-Gene assays. Genes were selected from a previous study that employed RNAseq to show that
545 cytoadhesion of two laboratory strains expressing different *Pf*EMP1 variants resulted in divergent
546 endothelial responses in TNF-activated HBMEC and identified differentially regulated pathways
547 implicated in CM pathology [25]. We found that IE from both UM and CM patient-derived parasite isolates
548 have differential effects on the HBMEC transcriptional response as compared to RBCs for 28 genes
549 (Supplementary Table 1 and Figure 2), but there was no difference when comparing UM with CM patient-
550 derived isolates (Figure 4). The UM and CM isolates were selected for this study based on their diverse
551 binding capacities to HBMEC and HDMEC from a previous study [26], and their ability to be established in
552 continuous culture to provide sufficient material for repeat experiments. Adapting *P. falciparum* patient
553 isolates to *in-vitro* culture requires considerable time, and thus *var* gene switching is likely to occur [44,53],
554 which was the case for some of the CM and UM isolates, as detected by qPCR (Supplementary Table 4).
555 This resulted in altered binding profiles to TNF-stimulated HBMEC with less distinction between the
556 isolates compared to that seen at the time of isolation from the patients, with exceptions of CM2 and CM4,

557 which still had relatively low and high binding to HBMEC, respectively (Figure 5). Binding to HDMEC
558 was not determined in this work for the cultured-adapted isolates, as the co-cultures were only performed
559 with HBMEC. Despite the variability in binding profiles, we observed important differences in the HBMEC
560 transcriptional response to IE compared to RBC in our *in vitro* model, supporting a role for PfEMP1 in
561 shaping the endothelial response to sequestration.

562

563 Comparing the binding capacity of each isolate to the relative gene expression of HBMEC after 6-hours
564 co-culture detected no significant correlation between the parasites' propensity to bind and the HBMEC
565 gene expression of *PTGIS*, *PTGS2* or *KL4* (Supplementary Figure 1). Furthermore, experiments performed
566 using the SBP1-KO parasite line revealed that there were no differences in the HBMEC responses to
567 binding and non-binding IE for these genes (Supplementary Table 2), yet there was a significant difference
568 in the magnitude of these responses between these two groups for 30 genes (Supplementary Table 3). SBP1-
569 KO parasites do not cytoadhere to HBMEC as they are unable to traffic PfEMP1 to the surface, although
570 they maintain both Maurer's cleft and knob morphology and the and expression of other Maurer's cleft-
571 associated proteins essential for tracking and IE surface changes, such as KAHRP, MAHRP, REX, PfEMP3,
572 and Pf332 [27,46]. RIFINs and STEVORs are proteins that are expressed on the surface of IE that are involved
573 in cytoadherence to RBC (rosetting) and immune cells [54], and their trafficking and expression is maintained
574 in SBP1-KO parasites [55]. Possemiers et al investigated sequestration-deficiency in experimental
575 *Plasmodium berghei* malaria-associated acute respiratory distress syndrome, and they observed endothelial
576 activation in SBP1-KO infected mice to the same level as wild type at eight days post infection in the lungs
577 [56]. Overall, SBP1-KO IE maintain an altered surface, including knobs, and can interact with HBMEC
578 differently compared to RBC. Our findings suggest that the interaction between HBMEC and IE via
579 PfEMP1 is not the only driver and that the observed differences in HBMEC relative gene expression are
580 also related to contact with intact parasitised RBC.

581

582 Homeostasis of the brain microvasculature is maintained by a delicate balancing of apoptosis, repair,
583 inflammation, and activation. We observed upregulation in the relative gene expression of HBMEC after
584 incubation with IE in a panel of genes, particularly in genes involved in apoptosis and the regulation of
585 inflammation and endothelial integrity. Overall, the fold change expression levels were relatively low,
586 except for the ones highlighted for further study and discussion. Expression of *BCL2A1* was increased and
587 a more robust *BCL2A1* expression was observed in HBMEC co-cultured with binding IE, as compared to
588 non-binding SBP1-KO (Supplementary Table 2). BCL2A1 is a member of the BCL2 pro-survival protein
589 family that regulates apoptosis by preventing activation of BAX and BAK, therefore inhibiting the

590 activation of the caspase cascade via caspase 9 [31]. However, adhesion of IE was also shown to induce
591 caspase 8- and caspase 9- dependent apoptosis [57]. Perhaps expression of *BLC2A1* early during an infection
592 represents the balance between protection and pathology and demonstrates the temporal kinetics in this
593 complicated system. As shown in Figure 1, CYP1A1, PTGIS, and PTGS2 are involved in lipid metabolism,
594 including the biosynthesis of prostacyclin, which has roles as an inflammatory mediator and a potent
595 vasodilator [41,58]. Despite observing transcriptional upregulation of *PTGIS* and *PTGS2*, FC±SEM of
596 2.05±0.24 and 4.92±0.26 respectively (Supplementary Table 2), this did not seem to translate into detection
597 of PTGS2 protein or 6-keto PGF1α (prostacyclin's stable hydrolysis product) in HBMEC lysate and co-
598 culture supernatant, respectively (Supplementary Table 5). PTGS2, or COX-2, is intracellularly localised,
599 and expression in cell lysates is usually detected by Western blot. To quantify PTGS2 concentrations in
600 multiple samples, an ELISA was chosen. Unfortunately, the usability of the ELISA kit was questionable, as
601 the positive control, stimulation with TNF, did not result in increased PTGS2 production. Therefore,
602 detection of PTGS2 was not pursued further. 6-keto PGF1α is secreted, and larger amounts were produced
603 upon stimulation with TNF and thrombin, but overall, no significant increase in production was detected
604 for the HBMEC-IE co-cultures compared to their respective HBMEC-RBC co-cultures. KLF2 and KLF4
605 are transcription factors that have been shown to directly regulate endothelial function and integrity in
606 vascular endothelium and to protect against endothelial dysfunction, both *in vitro* and in murine models
607 [36,37,39,59,60]. Overexpression of *KLF2* and *KLF4* affect coagulation and inflammatory pathways by inducing
608 expression and activity of endothelial nitric oxide synthase and thrombomodulin [37,39,40,59], while
609 simultaneously inhibiting expression of adhesion molecules E-selectin, ICAM-1, and VCAM-1 [39]. We
610 observed significant upregulation in relative gene expression of both *KLF2* and *KLF4* in HBMEC incubated
611 with IE. It would be interesting to further explore the modulation of gene and protein expression of KLF2
612 and KLF4 in this co-culture model over an extended period, as well as the temporal dynamics of these
613 transcription factors and the expression of adhesion molecules. Overall, our findings provide additional
614 evidence that IE regulate brain ECs and that these effects are not only due to binding.

615

616 Previous studies have investigated the effects of IE on endothelial responses *in vitro*. An investigation by
617 Zuniga et al examined how TNF and IE differently affected transcriptional responses and barrier integrity
618 in brain endothelial cells. Their work highlighted that TNF and IE lysates induce distinct transcriptional
619 profiles, with TNF associated with induction of endothelial activation while IE lysate contributed
620 considerably to endothelial barrier disruption, yet overlap in genes associated with inflammation, including
621 induction of PTGS2, were detected [23]. Howard et al adapted a 3D perfusion human brain microvessel model
622 to evaluate the brain endothelial responses to perfusion with TNF and at different stages of parasite

623 maturation. This study found that treatment of brain microvessels with TNF induced an inflammatory
624 phenotype, while EPCR-binding parasites caused localised barrier damage, and induced unique stress
625 response pathways associated with metal toxicity and oxidative stress [43]. Additionally, the sequential
626 treatment of 3D microvessels with TNF followed by IE revealed that binding of IE delayed endothelial cell
627 recovery and augmented TNF temporal kinetics. In concordance with Zuniga et al and Howard et al [23,43],
628 we observed that there is a group of inflammatory associated genes that are upregulated in HBMEC by
629 exposure to patient-derived IE and that this effect is independent of TNF treatment. This upregulation in
630 HBMEC relative gene expression was detected after 6-hours incubation with trophozoite-stage IE, in
631 contrast to previous studies that used schizont-stage IE or IE lysates for longer periods ranging from 6, 9,
632 12, and 24 hours [23,43]. In contrast to studies that use IE lysates and longer time courses [23,43,51], we utilised
633 trophozoite-IE prepared in EGM2min medium for a 6-hour incubation period. This medium maintains
634 HBMEC over the time course, but affects the progress of IE, as they barely develop beyond the trophozoite
635 stage. In our study we detect HBMEC effects at early stages of sequestration where IE are still in contact
636 with the endothelium, as opposed to effects attributed to parasite material and ruptured IE. An extended co-
637 culture time frame would have allowed us to observe other, perhaps larger, effects on HBMEC transcription.
638
639 The Fluidigm panel did not contain many cytokine genes and thus a multiplex assay was used to detect 41
640 cytokines in the co-culture supernatant. HBMEC produce low levels of cytokines in their basal state, and
641 this is not much increased after co-culture with IE, with a relatively low FC comparing IE to RBC co-
642 culture. Out of the 41 cyto/chemokines, 13 had concentrations exceeding 5 pg/ml and only a few of these
643 were significantly increased after co-culture with IE, compared to co-culture with their respective RBC
644 (Supplementary Table 6). The multiplex was performed at an early stage of the study and was not performed
645 with all the isolates or SBP1-KO, and only performed with one experiment, thus, the results are only an
646 indication of the effects of IE co-culture. Stimulation with TNF, as positive control, did increase the
647 concentrations of multiple cytokines, including IL-6, IL-8, IP-10 and MCP-1, also reported in other studies
648 [23,51,61]. Indeed, Zuniga et al[23] noted they observed transcriptionally similar but translationally different levels
649 of cytokines between their treatment groups even when total protein synthesis levels were similar,
650 suggesting a role for post-translational regulation in HBMEC after incubation with IE.
651
652 Whether the patient isolates affect HBMEC barrier integrity was determined by TEER with cell index as
653 measure of integrity. In all experiments the cell index was increased after adding IE, but to a similar level
654 as RBC, likely to be due to the layer of RBC on top of the HBMEC affecting conductivity (Supplementary
655 Figure 3A and B). None of the isolates decreased the HBMEC barrier function, even after 24 hours
656 (Supplementary Figure 3B). This contrasts with other studies where the addition of IE decreased the barrier

657 integrity [23,51] and is likely related to their use of schizont-stage IE or IE lysates, while trophozoite-stage IE
658 were used in our experiments. After 24 hours, parasites seemed to be in a resting stage and were not
659 progressing to schizont stage, therefore not releasing parasite factors, previously identified as the reason for
660 the decrease in barrier function [23,51,62].
661
662 It has been reported that IE affect the endothelial responses to thrombin [23,51], which reduces barrier function
663 rapidly and recovers within 2 hours. The presence of RBC or IE affected the response of HBMEC to
664 thrombin with a reduced maximum response and AUC, compared to medium (Supplementary Figures 3E
665 and F). There were no significant differences between RBC or IE, but there seemed a trend with IE at 30%
666 parasitaemia further reducing the effects of thrombin and this was the case for all the patient isolates. The
667 non-binding lab isolate SBP1-KO had almost identical effects as RBC at the three different parasitemias,
668 which were significantly different to the effect of 30% IE (Supplementary Figure 3D, E, and F), indicating
669 that receptor binding may be required to reduce the effect of thrombin. In contrast, Avril et al showed that
670 schizont IE, but not trophozoite IE, prolonged thrombin-induced barrier disruption, compared to RBC [51].
671 However, thrombin was added 2 – 3 hours after adding IE or RBC and not compared to the effect of
672 thrombin in medium. Thrombin decreases endothelial barrier function by cleavage of Protease Activated
673 Receptor 1 (PAR1) and involves the thrombomodulin /activated protein C system in which the balance of
674 thrombin and activated protein C determines PAR1-dependent barrier disruptive or protective action,
675 respectively [14,63]. The reduced effect of thrombin indicates a shift towards more activated protein C, which
676 was not investigated in this study. However, binding of IE to HBMEC induces receptor shedding and this
677 could change the level of thrombomodulin and endothelial protein C receptor, the receptors for thrombin
678 and protein C, respectively [62,64], affecting PAR1 cleavage. The TEER data show that specific binding of IE
679 to HBMEC do affect certain endothelial responses, not captured in the RNA transcription data.
680
681 One limitation of this study was the use of a 2-dimensional co-culture model that simplified the
682 heterogeneous and complex microvascular system down to static interaction between parasitized
683 erythrocytes and microvascular brain endothelium. Nonetheless, this model allowed for the study of the
684 HBMEC transcriptional response to patient-derived parasites and to assess if these responses were
685 dependent on IE cytoadhesion or clinical syndrome. In this model, HBMEC were stimulated with TNF
686 overnight before the cytokine stimuli was removed and the IE introduced for 6-hours co-culture. The ratio
687 of 110 IE/HBMEC in our experiments is similar to the range employed in other studies [23,51], which was
688 calculated in Zuniga et al to be equivalent to approximately two layers of IE on top of the HBMEC. We
689 validated whether the Fluidigm panel would reflect gene expression changes in the co-culture model by
690 exposing HBMEC overnight to IL-1beta and TNF and comparing the gene expression with a media control

691 (Table 1). We observed massive upregulation in HBMEC expression of several genes, including *CXCL3*,
692 *ICAM1*, *PTGS2*, *SELE*, and *VCAM1*, after incubation with both stimuli, confirming that our model was able
693 to determine regulation of specific genes. Furthermore, there was significant reduction in relative gene
694 expression after withdrawal of TNF from HBMEC (Figure 3). Overall, these findings suggest that the
695 changes in relative gene expression observed in HBMEC exposed to both binding and non-binding parasites
696 are due to the impact of IE.

697

698 During early stages of sequestration, we observed effects on endothelium that are both dependent and
699 independent of *Pf*EMP1. These effects were relatively small except for several genes, including *CYP1A1*,
700 *KLF4*, and *PTGS2*. These genes may represent early endothelial protective responses that act through
701 vascular regulation and modulation of thrombomodulin. There was no difference in gene regulation in
702 HBMEC based on the origin of the isolate nor the parasite binding capacities. Overall, interaction of IE and
703 endothelial cells in early stages of sequestration does induce some endothelial responses, including some
704 that are independent of PfEMP1, and this is the first investigation to our knowledge to study how non-
705 *Pf*EMP1 expressing IE affect endothelial transcriptional responses. Understanding the different
706 mechanisms of crosstalk between *P. falciparum* infected erythrocytes and host endothelium may help us to
707 develop interventions that support patients with severe malaria while effective anti-parasite drugs clear the
708 infection.

709

710 **Acknowledgements:** We thank the members of staff in the NGS facility at the Bioscience Core Labs in
711 KAUST for the training and use of the Fluidigm Biomark HD system. This work was supported by
712 Competitive Research Grant (CRG) to AP and AGC (Grant number: CRG6-3392.02) by the Office of
713 Sponsored Research (OSR) at the King Abdullah University of Science and Technology (KAUST). The
714 funder had no role in study design, data collection, or preparation of the manuscript.

715

716 **Author Contributions:** Study conceptualisation: AGC; funding acquisition and administration: AGC, AP;
717 study supervision: AGC, AP, JS; study investigation: CA, JS, GC; formal analysis: CA, JS; writing –
718 original draft: CA, JS; writing – review and editing: CA, JS, AGC, AP.

Supplementary Data

Supplementary Table 1: **Relative gene expression of HBMEC co-cultured with IE or with the corresponding RBC control for each gene in the panel.** Samples were collected after a 6-hour co-culture, and relative gene expression was calculated using the ΔΔCt method using GAPDH as the endogenous control and the corresponding experimental 6-hour HBMEC-media sample as the reference sample (baseline is FC =1). The mean Fold Change (FC) and standard error of the mean (SEM) for each gene were calculated using the technical triplicates of the two biological replicates (UM = uncomplicated malaria patient-derived isolates, CM = cerebral malaria patient-derived isolates, n = sample size). Highlighted rows have FC>1.5 for one of the IE groups. P-value summary defined= *,0.01-0.05; **, 0.001-0.01; ***, 0.0001-0.001; ****, <0.0001.

	WELCH'S T-TEST COMPARING HBMEC-RBC (N=21) AND HBMEC-UM (N=24) RELATIVE FC				**WELCH'S T-TEST COMPARING HBMEC-RBC (N=21) AND HBMEC-CM (N=24) RELATIVE FC**			
GENE	HBMEC-RBC(UM) mean FC ± SEM	HBMEC-UM mean FC ± SEM	P value	P value summary	HBMEC-RBC(CM) mean FC ± SEM	HBMEC-CM mean FC ± SEM	P value	P value summary
ACTB	1.01 ± 0.026	1.12 ± 0.053	0.0039	**	0.94 ± 0.02	1.23 ± 0.047	<0.0001	****
ACTG1	1.03 ± 0.028	1.25 ± 0.033	<0.0001	****	1.01 ± 0.021	1.29 ± 0.046	<0.0001	****
ADAM10	1.01 ± 0.016	1.16 ± 0.031	0.0002	***	1 ± 0.021	1.13 ± 0.028	0.0012	**
ADAM17	0.92 ± 0.04	1.14 ± 0.025	<0.0001	****	0.91 ± 0.027	1.1 ± 0.04	0.0002	***
ANGTP2	1.05 ± 0.037	0.9 ± 0.025	0.0014	**	1.09 ± 0.021	0.96 ± 0.043	0.0075	**
ANK1	0.84 ± 0.049	0.99 ± 0.087	0.1365	ns	0.91 ± 0.086	1.22 ± 0.17	0.1132	ns
BAX	0.97 ± 0.028	0.98 ± 0.031	0.8577	ns	0.97 ± 0.022	1 ± 0.024	0.2942	ns
BCL2A1	1.03 ± 0.078	2.25 ± 0.093	<0.0001	****	1.03 ± 0.064	2.55 ± 0.171	<0.0001	****
CASP3	1.05 ± 0.041	1.07 ± 0.064	0.7753	ns	1.01 ± 0.03	0.98 ± 0.041	0.6767	ns
CCL14	0.96 ± 0.038	0.67 ± 0.035	<0.0001	****	1 ± 0.039	0.78 ± 0.031	0.0001	***
CDH5	0.99 ± 0.022	1.02 ± 0.022	0.3607	ns	0.96 ± 0.024	1 ± 0.013	0.1881	ns
CXCL3	0.79 ± 0.106	1.82 ± 0.26	0.0009	***	0.86 ± 0.097	1.72 ± 0.184	0.0002	***
CYP1A1	4.6 ± 0.374	10.46 ± 1.388	0.0004	***	5.32 ± 0.299	11.39 ± 0.838	<0.0001	****
DUSP5	0.96 ± 0.032	1.52 ± 0.048	<0.0001	****	0.91 ± 0.045	1.44 ± 0.069	<0.0001	****
EEF1A1	1.01 ± 0.056	1.21 ± 0.058	0.0195	*	0.97 ± 0.04	1.22 ± 0.06	0.0012	**
FAS	0.96 ± 0.058	0.96 ± 0.072	0.9836	ns	1.02 ± 0.057	0.94 ± 0.048	0.302	ns
HES1	1.05 ± 0.043	1.32 ± 0.075	0.004	**	1.02 ± 0.045	1.28 ± 0.088	0.0135	*
HEY1	0.81 ± 0.055	0.84 ± 0.054	0.7524	ns	0.73 ± 0.045	0.74 ± 0.048	0.8462	ns
HEY2	1.38 ± 0.123	1.24 ± 0.118	0.4226	ns	1.43 ± 0.116	1.38 ± 0.138	0.7798	ns
ICAM1	1 ± 0.109	1.39 ± 0.144	0.0358	*	0.97 ± 0.109	1.41 ± 0.116	0.0088	**
IL1A	1.21 ± 0.085	1.92 ± 0.106	<0.0001	****	1.27 ± 0.084	1.99 ± 0.112	<0.0001	****
IL6	1.16 ± 0.062	1.39 ± 0.053	0.0079	**	1.01 ± 0.033	1.59 ± 0.103	<0.0001	****
KLF10	1.04 ± 0.031	1.17 ± 0.071	0.0986	ns	0.97 ± 0.037	1.02 ± 0.057	0.4834	ns
KLF2	1.03 ± 0.039	1.82 ± 0.079	<0.0001	****	0.96 ± 0.029	1.73 ± 0.096	<0.0001	****
KLF3	0.93 ± 0.065	1.02 ± 0.033	0.2563	ns	0.89 ± 0.039	1 ± 0.031	0.0452	*
KLF4	0.86 ± 0.089	3.08 ± 0.339	<0.0001	****	0.77 ± 0.061	2.67 ± 0.208	<0.0001	****
LAMC2	1 ± 0.034	1.14 ± 0.034	0.0039	**	0.98 ± 0.038	1.2 ± 0.051	0.0016	**
MIB1	1.09 ± 0.034	1.31 ± 0.047	0.0005	***	0.98 ± 0.039	1.26 ± 0.046	<0.0001	****
NFKB1	1 ± 0.039	1.1 ± 0.059	0.1724	ns	0.93 ± 0.031	0.94 ± 0.038	0.8053	ns
NFKBIA	0.81 ± 0.057	0.9 ± 0.053	0.2358	ns	0.82 ± 0.057	0.87 ± 0.045	0.4546	ns

NOTCH2	1.04 ± 0.104	1.16 ± 0.105	0.4248	ns	1.03 ± 0.109	1.48 ± 0.197	0.054	ns
OCLN	0.97 ± 0.081	0.87 ± 0.072	0.3534	ns	0.9 ± 0.061	1.02 ± 0.047	0.1321	ns
PAPLN	1.1 ± 0.082	1.53 ± 0.095	0.0013	**	1.07 ± 0.073	1.47 ± 0.127	0.01	**
PECAM1	0.92 ± 0.027	1.08 ± 0.033	0.0006	***	0.92 ± 0.019	1.07 ± 0.024	<0.0001	****
PLA2G4A	1.23 ± 0.071	1.49 ± 0.095	0.0336	*	1.04 ± 0.06	1.3 ± 0.078	0.0113	*
PLXNA4	1.44 ± 0.318	1.37 ± 0.308	0.8739	ns	1.24 ± 0.314	1.35 ± 0.285	0.8057	ns
PROCR	1.03 ± 0.024	1.22 ± 0.04	0.0002	***	0.99 ± 0.029	1.25 ± 0.052	<0.0001	****
PTGIS	1.04 ± 0.122	2.07 ± 0.284	0.0022	**	1.52 ± 0.255	2.02 ± 0.391	0.2894	ns
PTGS2	1.54 ± 0.153	4.69 ± 0.275	<0.0001	****	1.51 ± 0.048	5.15 ± 0.431	<0.0001	****
S100A10	0.92 ± 0.026	1 ± 0.029	0.0526	ns	0.94 ± 0.019	1.04 ± 0.019	0.0007	***
SELE	0.72 ± 0.111	0.78 ± 0.111	0.7099	ns	0.87 ± 0.125	1.46 ± 0.135	0.0023	**
SMAD6	1.4 ± 0.099	1.66 ± 0.125	0.1028	ns	1.14 ± 0.097	1.82 ± 0.178	0.0019	**
TGFB1	1 ± 0.033	1.17 ± 0.045	0.0039	**	0.94 ± 0.027	1.11 ± 0.039	0.0013	**
TJP1	0.99 ± 0.031	0.93 ± 0.032	0.1611	ns	0.9 ± 0.031	0.93 ± 0.03	0.4792	ns
TNFRSF12A	1.31 ± 0.084	1.3 ± 0.147	0.9386	ns	1.14 ± 0.105	1.08 ± 0.089	0.626	ns
TSPAN13	0.96 ± 0.052	1.1 ± 0.052	0.0645	ns	0.93 ± 0.049	1.06 ± 0.04	0.0457	*
TUBB	1.02 ± 0.02	1.02 ± 0.026	0.9383	ns	0.98 ± 0.016	1.05 ± 0.02	0.0115	*
TXNIP	1.47 ± 0.165	2.63 ± 0.485	0.0311	*	0.98 ± 0.054	2.9 ± 0.64	0.0064	**
VCAM1	0.83 ± 0.083	1.78 ± 0.121	<0.0001	****	0.85 ± 0.087	2.06 ± 0.252	<0.0001	****

727

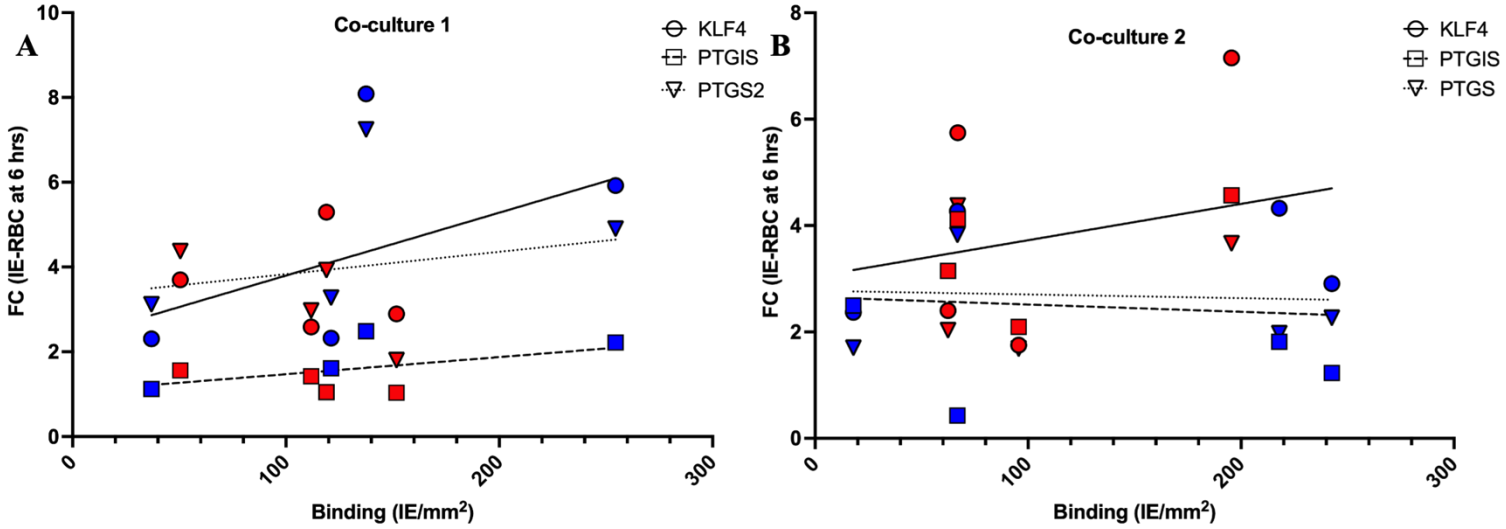

Supplementary Figure 1: **Binding capacities of patient-derived parasite isolates do not correlate with HBMEC gene expression.** The binding capacity of each isolate (IE/ mm^2) was compared to the 6-hour HBMEC mean FC relative gene expression for select genes (red = UM isolates; blue = CM isolates) after the first (A) and second (B) experiments using a linear regression. The linear regression for KLF4, PTGIS, and PTGS2 are indicated on each graph by straight, dashed, and dotted lines, respectively, and the R^2 values are reported as follows: Co-culture 1) KLF4 = 0.22, PTGIS= 0.25, PTGS2= 0.05; Co-culture 2) KLF4 = 0.10, PTGIS= 0.01, PTGS2= 0.003. Relative gene expression was calculated for HBMEC-IE using the ΔΔCt method with GAPDH as the endogenous control and the corresponding 6-hour HBMEC-RBC as the reference sample (baseline is FC=1). Each point represents the mean FC for each HBMEC-IE sample (n=8), calculated from the technical triplicates. Pearson's correlation was performed to compare parasite binding capacity to the differential gene expression for each isolate for both experiments, and the correlation coefficient (r) values are reported as follows: Co-culture 1) KLF4 = 0.47, PTGIS= 0.50, PTGS2= 0.22; Co-culture 2) KLF4 = 0.31, PTGIS= -0.08, PTGS2= -0.05.

Supplementary Table 2: **Relative gene expression of HBMEC co-cultured with binding or non-binding IE compared to the corresponding HBMEC-RBC control for each gene in the panel.** All samples were from a 6-hour time point. Data from UM and CM patient parasite isolates were combined to form a group of binding parasites, while two experiments with non-binding SBP1KO parasites were performed. Relative gene expression was calculated using the ΔΔCt method using GAPDH as the endogenous control and the corresponding experimental 6-hour HBMEC-media sample as the reference sample (baseline is FC=1). The mean Fold Change (FC) and standard error of the mean (SEM) for each gene were calculated using all experimental samples and technical replicates (SBP1KO= SBP1-knockout parasites, n = sample size). Highlighted rows have FC>1.5 for one of the HBMEC groups. P-value summary defined= *,0.01-0.05; **, 0.001-0.01; ***, 0.0001-0.001; ****, <0.0001.

	WELCH'S T-TEST COMPARING HBMEC-RBC (N=30) AND HBMEC-BINDING (N=48) RELATIVE FC				**WELCH'S T-TEST COMPARING HBMEC-RBC (N=6) AND HBMEC-SBP1KO (N=6) RELATIVE FC**			
GENE	HBMEC-RBC mean FC ± SEM	HBMEC-binding mean FC ± SEM	P value	P value summary	HBMEC-RBC mean FC ± SEM	HBMEC-SBP1KO mean FC ± SEM	P value	P value summary
ACTB	0.97 ± 0.022	1.21 ± 0.035	<0.0001	****	0.96 ± 0.035	1.06 ± 0.02	0.0372	*
ACTG1	1.01 1.01 ± 0.021	1.27 ± 0.028	<0.0001	****	0.95 ± 0.035	0.98 ± 0.032	0.6649	ns
ADAM10	1.01 ± 0.016	1.14 ± 0.021	<0.0001	****	0.88 ± 0.044	1.03 ± 0.04	0.0299	*
ADAM17	0.93 ± 0.03	1.12 ± 0.023	<0.0001	****	0.87 ± 0.036	1.05 ± 0.033	0.0045	**
ANGTP2	1.06 ± 0.027	0.93 ± 0.025	0.0007	***	1.01 1.01 ± 0.025	0.94 ± 0.04	0.1918	ns
ANK1	0.88 ± 0.065	1.1 ± 0.096	0.0535	ns	0.83 ± 0.184	0.83 ± 0.098	0.9934	ns
BAX	0.98 ± 0.02	0.99 ± 0.019	0.7438	ns	0.96 ± 0.05	0.81 ± 0.039	0.0424	*
BCL2A1	0.97 ± 0.057	2.4 ± 0.099	<0.0001	****	1.01 ± 0.078	1.59 ± 0.058	0.0002	***
CASP3	1.02 ± 0.033	1.03 ± 0.038	0.8538	ns	0.94 ± 0.056	0.87 ± 0.059	0.3719	ns
CCL14	0.96 ± 0.031	0.73 ± 0.025	<0.0001	****	0.75 ± 0.06	0.48 ± 0.022	0.0052	**
CDH5	0.96 ± 0.019	1.01 ± 0.013	0.0399	*	0.98 ± 0.023	0.88 ± 0.016	0.0075	**
CXCL3	0.8 ± 0.075	1.77 ± 0.157	<0.0001	****	2.17 ± 0.371	2.89 ± 0.551	0.3076	ns
CYP1A1	4.94 ± 0.314	10.92 ± 0.805	<0.0001	****	5.54 ± 0.604	8.57 ± 1.017	0.0329	*
DUSP5	0.9 ± 0.033	1.48 ± 0.042	<0.0001	****	1.06 ± 0.111	2.11 ± 0.138	0.0002	***
EEF1A1	0.97 ± 0.042	1.22 ± 0.041	<0.0001	****	0.89 ± 0.06	0.84 ± 0.023	0.4657	ns
FAS	1 ± 0.05	0.95 ± 0.043	0.4783	ns	0.75 ± 0.079	0.69 ± 0.062	0.6216	ns
HES1	1.01 ± 0.034	1.3 ± 0.057	<0.0001	****	0.9 ± 0.036	1.47 ± 0.056	<0.0001	****
HEY1	0.79 ± 0.046	0.79 ± 0.037	0.8966	ns	0.76 ± 0.088	0.62 ± 0.04	0.1779	ns
HEY2	1.32 ± 0.095	1.31 ± 0.09	0.9267	ns	0.91 ± 0.202	1.47 ± 0.359	0.2132	ns
ICAM1	1 ± 0.08	1.4 ± 0.091	0.0016	**	1.24 ± 0.118	1.73 ± 0.293	0.1706	ns
IL1A	1.23 ± 0.063	1.95 ± 0.076	<0.0001	****	1.5 ± 0.095	1.91 ± 0.177	0.077	ns
IL6	1.11 ± 0.048	1.49 ± 0.059	<0.0001	****	1.32 ± 0.085	1.7 ± 0.149	0.0551	ns
KLF10	0.98 ± 0.029	1.09 ± 0.046	0.048	*	1.18 ± 0.112	1.3 ± 0.108	0.4584	ns
KLF2	1 ± 0.032	1.78 ± 0.062	<0.0001	****	1.01 ± 0.073	1.53 ± 0.12	0.0056	**
KLF3	0.94 ± 0.046	1.01 ± 0.022	0.1811	ns	0.9 ± 0.042	0.7 ± 0.032	0.005	**
KLF4	0.84 ± 0.069	2.87 ± 0.199	<0.0001	****	0.77 ± 0.098	1.58 ± 0.254	0.0239	*
LAMC2	0.99 ± 0.029	1.17 ± 0.031	<0.0001	****	1.12 ± 0.093	1.24 ± 0.142	0.482	ns
MIB1	1.04 ± 0.033	1.29 ± 0.033	<0.0001	****	0.73 ± 0.052	1.16 ± 0.046	0.0001	***
NFKB1	0.98 ± 0.03	1.02 ± 0.037	0.445	ns	0.79 ± 0.062	0.7 ± 0.059	0.2969	ns
NFKBIA	0.82 ± 0.041	0.89 ± 0.034	0.2302	ns	1.16 ± 0.085	1.13 ± 0.102	0.8297	ns

NOTCH2	1.05 ± 0.089	1.32 ± 0.113	0.0702	ns	1.6 ± 0.821	2.62 ± 1.152	0.4893	ns
OCLN	0.95 ± 0.058	0.94 ± 0.044	0.9851	ns	0.88 ± 0.084	0.92 ± 0.095	0.7435	ns
PAPLN	1.04 ± 0.065	1.5 ± 0.079	<0.0001	****	0.95 ± 0.149	1 ± 0.083	0.7714	ns
PECAM1	0.91 ± 0.02	1.07 ± 0.02	<0.0001	****	0.96 ± 0.034	0.91 ± 0.032	0.2936	ns
PLA2G4A	1.15 ± 0.057	1.4 ± 0.062	0.0046	**	1.31 ± 0.224	1.51 ± 0.173	0.4987	ns
PLXNA4	1.32 ± 0.225	1.36 ± 0.207	0.9008	ns	1.01 ± 0.267	0.58 ± 0.068	0.1718	ns
PROCR	0.99 ± 0.022	1.24 ± 0.033	<0.0001	****	0.89 ± 0.037	0.92 ± 0.033	0.5743	ns
PTGIS	1.35 ± 0.188	2.05 ± 0.239	0.0252	*	1.64 ± 0.367	1.84 ± 0.442	0.7465	ns
PTGS2	1.57 ± 0.107	4.92 ± 0.255	<0.0001	****	1.58 ± 0.144	6.57 ± 0.422	<0.0001	****
S100A10	0.93 ± 0.02	1.02 ± 0.017	0.001	**	0.93 ± 0.053	0.82 ± 0.045	0.1704	ns
SELE	0.88 ± 0.1	1.12 ± 0.1	0.0935	ns	1.45 ± 0.286	2.66 ± 0.298	0.0147	*
SMAD6	1.25 ± 0.082	1.74 ± 0.108	0.0005	***	1.74 ± 0.381	1.52 ± 0.178	0.6283	ns
TGFB1	0.97 ± 0.025	1.14 ± 0.03	<0.0001	****	0.93 ± 0.042	1.14 ± 0.065	0.0236	*
TJP1	0.94 ± 0.028	0.93 ± 0.022	0.7211	ns	0.85 ± 0.069	0.77 ± 0.048	0.3735	ns
TNFRSF12A	1.24 ± 0.087	1.19 ± 0.087	0.6808	ns	1.2 ± 0.184	0.84 ± 0.171	0.1886	ns
TSPAN13	0.93 ± 0.038	1.08 ± 0.033	0.0051	**	0.86 ± 0.044	0.84 ± 0.033	0.6971	ns
TUBB	1.01 ± 0.017	1.04 ± 0.016	0.2726	ns	0.88 ± 0.044	0.9 ± 0.036	0.8362	ns
TXNIP	1.29 ± 0.129	2.76 ± 0.397	0.0008	***	0.81 ± 0.11	0.98 ± 0.18	0.4599	ns
VCAM1	0.84 ± 0.065	1.92 ± 0.14	<0.0001	****	1.13 ± 0.067	3.84 ± 0.482	0.0023	**

Supplementary Table 3: **Comparing the relative gene expression of HBMEC co-cultured with either binding IE or non-binding IE for each gene in the panel.** All samples were from a 6-hour time point. Data from UM and CM patient parasite isolates were combined to form a group of binding parasites, while two experiments with non-binding SBP1KO parasites were performed. Relative gene expression was calculated using the ΔΔCt method using GAPDH as the endogenous control and the corresponding experimental 6-hour HBMEC-media sample as the reference sample (baseline is FC=1). The mean Fold Change (FC) and standard error of the mean (SEM) for each gene were calculated using all experimental samples and technical replicates (SBP1KO= SBP1-knockout parasites, n = sample size). Highlighted rows have FC>1.5 for one of the HBMEC groups. P-value summary defined= *,0.01-0.05; **, 0.001-0.01; ***, 0.0001-0.001; ****, <0.0001.

WELCH'S T-TEST COMPARING HBMEC-BINDING (N=48) AND HBMEC-SBP1KO (N=6) RELATIVE FC

GENE	HBMEC-binding mean FC ± SEM	HBMEC-SBP1KO mean FC ± SEM	P value	P value summary
ACTB	0.97 ± 0.022	1.21 ± 0.035	0.0004	***
ACTG1	1.02 1.01 ± 0.021	1.27 ± 0.028	<0.0001	****
ADAM10	1.01 ± 0.016	1.14 ± 0.021	0.0366	*
ADAM17	0.93 ± 0.03	1.12 ± 0.023	0.1025	ns
ANGTP2	1.06 ± 0.027	0.93 ± 0.025	0.7908	ns
ANK1	0.88 ± 0.065	1.1 ± 0.096	0.0647	ns
BAX	0.98 ± 0.02	0.99 ± 0.019	0.0039	**
BCL2A1	0.97 ± 0.057	2.4 ± 0.099	<0.0001	****
CASP3	1.02 ± 0.033	1.03 ± 0.038	0.0452	*
CCL14	0.96 ± 0.031	0.73 ± 0.025	<0.0001	****

CDH5	0.96 ± 0.019	1.01 ± 0.013	<0.0001	****
CXCL3	0.8 ± 0.075	1.77 ± 0.157	0.0993	ns
CYP1A1	4.94 ± 0.314	10.92 ± 0.805	0.0935	ns
DUSP5	0.9 ± 0.033	1.48 ± 0.042	0.0047	**
EEF1A1	0.97 ± 0.042	1.22 ± 0.041	<0.0001	****
FAS	1 ± 0.05	0.95 ± 0.043	0.0066	**
HES1	1.01 ± 0.034	1.3 ± 0.057	0.0401	*
HEY1	0.79 ± 0.046	0.79 ± 0.037	0.0062	**
HEY2	1.32 ± 0.095	1.31 ± 0.09	0.6924	ns
ICAM1	1 ± 0.08	1.4 ± 0.091	0.3252	ns
IL1A	1.23 ± 0.063	1.95 ± 0.076	0.8299	ns
IL6	1.11 ± 0.048	1.49 ± 0.059	0.2282	ns
KLF10	0.98 ± 0.029	1.09 ± 0.046	0.1196	ns
KLF2	1 ± 0.032	1.78 ± 0.062	0.1113	ns
KLF3	0.94 ± 0.046	1.01 ± 0.022	<0.0001	****
KLF4	0.84 ± 0.069	2.87 ± 0.199	0.0016	**
LAMC2	0.99 ± 0.029	1.17 ± 0.031	0.6425	ns
MIB1	1.04 ± 0.033	1.29 ± 0.033	0.0432	*
NFKB1	0.98 ± 0.03	1.02 ± 0.037	0.0012	**
NFKBIA	0.82 ± 0.041	0.89 ± 0.034	0.0636	ns
NOTCH2	1.05 ± 0.089	1.32 ± 0.113	0.3123	ns
OCLN	0.95 ± 0.058	0.94 ± 0.044	0.8125	ns
PAPLN	1.04 ± 0.065	1.5 ± 0.079	0.0004	***
PECAM1	0.91 ± 0.02	1.07 ± 0.02	0.0017	**
PLA2G4A	1.15 ± 0.057	1.4 ± 0.062	0.5597	ns
PLXNA4	1.32 ± 0.225	1.36 ± 0.207	0.0008	***
PROCR	0.99 ± 0.022	1.24 ± 0.033	<0.0001	****
PTGIS	1.35 ± 0.188	2.05 ± 0.239	0.6864	ns
PTGS2	1.57 ± 0.107	4.92 ± 0.255	0.0083	**
S100A10	0.93 ± 0.02	1.02 ± 0.017	0.0051	**
SELE	0.88 ± 0.1	1.12 ± 0.1	0.0025	**
SMAD6	1.25 ± 0.082	1.74 ± 0.108	0.3217	ns
TGFB1	0.97 ± 0.025	1.14 ± 0.03	0.9822	ns
TJP1	0.94 ± 0.028	0.93 ± 0.022	0.0189	*
TNFRSF12A	1.24 ± 0.087	1.19 ± 0.087	0.1105	ns
TSPAN13	0.93 ± 0.038	1.08 ± 0.033	<0.0001	****
TUBB	1.01 ± 0.017	1.04 ± 0.016	0.0091	**
TXNIP	1.29 ± 0.129	2.76 ± 0.397	0.0002	***
VCAM1	0.84 ± 0.065	1.92 ± 0.14	0.009	**

***Supplementary Table 4: var* genotyping of patient isolates after culturing by qPCR.** The primer sets detect multiple group A and A/B *var* domains and in addition the combined CIDRα1 domains were calculated. The transcript unit (Tu) was calculated for the patient isolates at the time of isolation (original) and after a number of days in culture (DIC). A Tu value of 1 equals low abundance transcript and a value of 32 equals transcript levels as the endogenous genes *seryl-tRNA synthetase* and *aldolase*. Nd: not determined. For a detailed description of the domains see Mkumbaye et al [65].

		UM1	**UM1**	**UM2**	**UM2**	**UM3**	**UM3**	**UM3**	**UM4**	**UM4**	**CM1**	**CM1**	**CM1**
Domain	**Group**	Original	42 DIC	Original	34 DIC	Original	33 DIC	42 DIC	Original	26 DIC	Original	28 DIC	29 DIC
CIDRα1.1	B/A	8	1	5	1	2	3	1	5	1	53	13	1
CIDRα1.8a	B/A	1	1	1	nd	1	1	1	nd	1	6	nd	1
CIDRα1.8b	B/A	1	1	1	1	1	1	1	nd	1	48	46	1
Sum: CIDRα1.DC8	B/A	8	1	5	1	2	3	1	5	1	107	59	1
CIDRα1.4	A	1	1	1	1	1	1	1	1	1	12	4	1
CIDRα1.5a	A	1	1	1	1	1	nd	1	1	1	33	53	1
CIDRα1.5b	A	4	3	2	1	1	1	1	3	1	1	1	1
CIDRα1.6a	A	1	1	1	1	1	1	1	nd	1	21	11	1
CIDRα1.6b	A	1	1	1	1	1	nd	1	nd	nd	1	3	nd
CIDRα1.7	A	4	1	2	1	5	1	1	1	1	2	23	1
Sum: CIDRα1.A	A	8	4	4	1	5	1	1	4	1	68	94	1
Sum:CIDRα1_all	A & B/A	16	5	8	1	7	3	1	10	1	175	154	1
DBLβ1/3-1	A	2	1	1	1	1	10	1	5	3	1	55	1
DBLβ1/3-2	A	9	1	3	1	12	17	1	613	341	19	815	1
DBLβ5	B	1	1	3	2	1	5	1	2	5	8	9	1
DC5	A	5	1	1	1	1	1	1	nd	3	66	86	1
CIDRα3.1/3.2	B/C	5	1	2	1	2	11	1	1	4	5	27	1
CIDRδ	A	2	1	1	1	3	4	2	nd	1	8	44	1
CIDRγ3.1	A	1	1	nd	1	1	1	1	nd	nd	1	1	nd
DBLα1all	A	26	3	10	2	7	21	1	296	222	104	220	1
DBLα2/1.1/1.2/1.4/1	A	36	5	33	11	11	10	2	109	73	185	383	4
DBLα1.5/1.6/1.8	A	20	1	4	1	5	12	2	6	2	65	48	1
CIDRα1.2-K		1	1	nd	1	1	nd	1	nd	nd	1	nd	nd
CIDRα1.2-		1	1	1	1	1	1	1	nd	1	3	2	1

CM2	Original	1	nd	nd	1	1	1	1	1	2	nd	nd	1	1	2	2	1	1	1	1	1	5	nd	nd	413	12	146	nd	nd
CM2	43 DIC	1	1	1	1	1	1	1	1	1	1	1	1	1	1	1	1	1	1	1	1	1	1	1	4	1	3	1	1
CM3	Original	no data																											
CM3	51 DIC	1	1	1	1	1	1	1	1	1	1	1	1	1	1	1	1	1	1	1	1	1	1	1	1	5	1	1	1
CM4	Original	52	1	1	1	52	3	1	1	7	7	1	2	19	72	6	1	2	7	33	2	7	3	1	47	156	47	1	1
CM4	33 DIC	2	1	1	1	2	1	1	1	1	1	nd	1	1	3	1	1	1	1	26	1	1	1	1	3	14	9	nd	1

Supplementary Table 5: **Determination of prostaglandin endoperoxide synthase 2 (PTGS2) and prostacyclin production in HBMEC-IE co-cultures by ELISA.** Prostacyclin has a short half-life and therefore its hydrolysis product, 6-keto prostaglandin F1α (6-keto PGF1α), was detected in culture medium after co-culture with IE or RBC. PTGS2 was detected in HBMEC cell lysate after co-culture and calculated as ng PTGS2 per mg total lysate protein. The mean ± SD of 2 technical replicates is shown and per experiment the ratio of the enzyme concentrations for HBMEC-IE and HBMEC-RBC was calculated. 4 UM isolates, 4 CM isolates and SBP1-KO were co-cultured for 6 hours and for the CM4 isolate and SBP1-KO a co-culture of 20 hours was also performed (experiment 12 and 13). As control, HBMEC were incubated with 10 ng/ml TNF for 6 (experiment C2) and 20 hours (experiment C2 and C3). Thrombin is a fast-acting stimulator of prostacyclin production and the concentration of 6-keto PGF1α was detected in HBMEC after 15- and 30-minutes incubation with 5 nM thrombin (experiment C3). Statistical significance between HBMEC-IE and corresponding HBMEC-RBC and or control condition and medium was determined by unpaired t-test with Welch correction with * p-value < 0.05 and ** p-value < 0.01.

		[6ketoPGF1α] pg/ml		**[PTGS2] ng/mg protein**	
Exp	**Condition**	**Mean ± SD**	**IE/RBC**	**Mean ± SD**	**IE/RBC**
1	6h RBC	608 ± 43			
1	6h UM3-1	996 ± 136	1.64		
1	6h UM3-2	1046 ± 13 *	1.72		
1	6h CM2	1153 ± 271	1.90		
2	6h RBC	1621 ± 390			
2	6h UM1	952 ± 133	0.59		
2	6h CM3	1256 ± 162	0.77		
3	6h RBC	1679 ± 208			
3	6h CM1-1	1505 ± 73	0.90		
3	6h CM1-2	1611 ± 320	0.96		
4	6h RBC	437 ± 38			
4	6h UM2	803 ± 22 *	1.84		
5	6h RBC	664 ± 10		16.2 ± 0.3	
5	6h CM3	358 ± 100	0.54	19.1 ± 1.2	1.2
5	6h UM1	434 ± 56	0.65	10.8 ± 1.7	0.7

6	6h RBC	772 ± 182		18.0 ± 1.0	
6	6h CM4	694 ± 105	0.90	11.4 ± 0.6 *	0.6
7	6h RBC	1309 ± 265		19.0 ± 2.4	
7	6h UM3	1018 ± 79	0.78	10.0 ± 0.2	0.5
8	6h RBC	1194 ± 46		21.0 ± 0.6	
8	6h UM2	5720 ± 1378	4.79	17.4 ± 1.2	0.8
9	6h RBC	396 ± 19		19.4 ± 1.1	
9	6h CM1	695 ± 12 **	1.75	13.2 ± 1.3 *	0.7
10	6h RBC	1595 ± 114			
10	6h UM4	2013 ± 244	1.26		
11	6h RBC	4192 ± 1			
11	6h SBP1-KO-1	7213 ± 561	1.72		
12	6h RBC	1423 ± 109		13.7 ± 0.1	
12	6h CM4	1871 ± 98	1.32	12.5 ± 2.4	0.9
12	20h RBC	3754 ± 170		14.2 ± 1.5	
12	20h CM4	7382 ± 1233	1.97	9.0 ± 1.4	0.6
13	6h RBC	651 ± 11		15.3 ± 0.7	
13	6h SBP1-KO	480 ± 165	0.74	14.4 ± 2.1	0.9
13	20h RBC	2729 ± 113		13.2 ± 1.0	
13	20h SBP1-KO	8526 ± 1295	3.12	11.6 ± 3.1	0.9
C1	30 min medium	100 ± 0			
C1	15 min thrombin (5 nM)	1071 ± 104 *	10.74		
C1	30 min thrombin (5 nM)	826 ± 156	8.29		
C2	6h medium	264 ± 0			
C2	6h TNF (10 ng/ml)	909 ± 62 *	3.44		
C2	20h medium	685 ± 152			
C2	20h TNF (10 ng/ml)	2234 ± 1374	3.26		
C3	20h medium	178 ± 13		123.7 ± 14.9	
C3	20h TNF (10 ng/ml)	1200 ± 70 *	6.73	118.5 ± 19.4	1.0

766

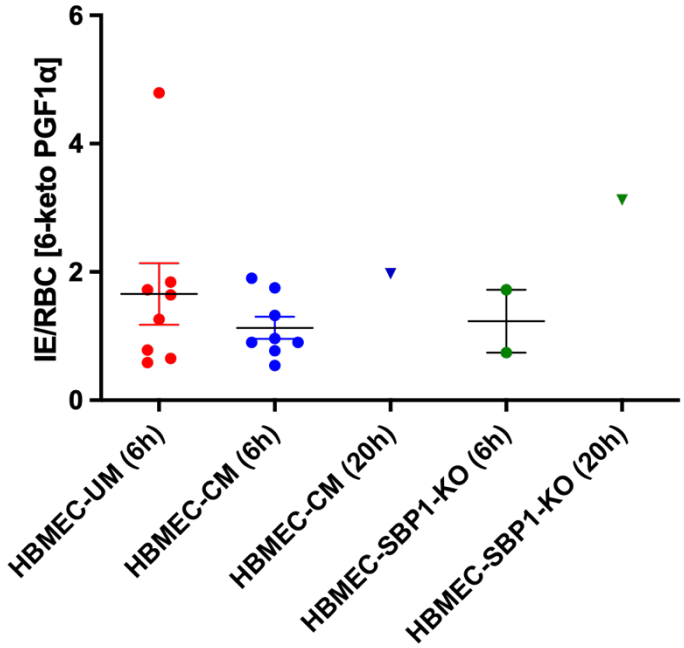

Supplementary Figure 2: **Ratio of 6-keto prostaglandin F1α concentrations in HBMEC-IE and HBMEC-RBC co-cultures.** 6-keto PGF1α was detected in culture medium after co-culture with IE or RBC and per experiment the ratio of the enzyme concentrations for HBMEC-IE and HBMEC-RBC was calculated (data in Supplementary Table 4). Plotted are mean ± SD of the ratios for the co-cultures with CM and UM isolates and the SBP1-KO strain.

Supplementary Table 6: **Production of cytokines and chemokines in HBMEC-IE co-cultures.** A panel of 41 secreted cytokines and chemokines were measured in the co-culture medium of 6 hours co-culture of HBMEC-IE and HBMEC-RBC by Luminex. The results (pg/ml) are shown for 13 cytokines of which the concentration was higher than 5 pg/ml for 3 CM isolates, 2 UM isolates and 2 lab strains: IT4var14 and IT4var37. A positive control of HBMEC activated by 10 ng/ml TNF for 16 hours was included. The mean ± SD of two technical replicates is shown with significance between HBMEC-IE and HBMEC-RBC calculated by unpaired t-test with Welch correction, with * p-value < 0.05, ** p-value < 0.01 and *** p-value <0. 001.The ratio of the values of HBMEC-IE and HBEC-RBC was calculated per experiment. Note that the CM5 isolate was only included in this multiplex experiment and was not part of all the other experiments described.

	G-CSF	GM-CSF	Fractalkine	IFNg
6h RBC	120 ± 10	10 ± 1	165 ± 32	0.7 ± 0.5
6h CM1	136 ± 10	13 ± 0	102 ± 0	8.0 ± 0.6 **
IE/RBC	1.1	1.2	0.6	10.8
6h RBC	369 ± 30	29 ± 2	341 ± 45	0.7 ± 0.0
6h CM4	656 ± 14	49 ± 0.1	219 ± 22	7.4 ± 1.5
IE/RBC	1.8	1.7	0.6	10.0
6h RBC	423 ± 42	32 ± 0	343 ± 10	1.2 ± 0.4
6h CM5	715 ± 6	49 ± 3	161 ± 13 **	2.9 ± 0.6
IE/RBC	1.7	1.5	0.5	2.5
6h UM3	805 ± 29	38 ± 2	137 ± 20 *	4.6 ± 0.0 *
IE/RBC	1.9	1.2	0.4	3.9
6h RBC	151 ± 5	19 ± 1	195 ± 24	1.1 ± 0.0
6h UM2	213 ± 1	29 ± 1	107 ± 7	5.4 ± 0.2 *
IE/RBC	1.4	1.5	0.6	5.0
6h RBC	57 ± 2	9 ± 1	128 ± 7	1.3 ± 0.2
6h Var37	61 ± 4	9 ± 1	105 ± 11	2.3 ± 0.2
IE/RBC	1.1	1.0	0.8	1.8
6h RBC	212 ± 16	18 ± 0.3	120 ± 11	1.1 ± 0.5
6hVar14	328 ± 22	26 ± 3	71 ± 13	1.6 ± 0.2
IE/RBC	1.5	1.4	0.6	1.5
medium overnight	36 ± 0	1 ± 0.3	23 ± 17	0.4 ± 0
TNF overnight	nd	1385 ± 17 **	2227 ± 25 ***	1.6 ± 0.2
TNF/medium		1372	190	4

GRO	PDGF-AA	IL-4	IL-6	IL-8	IP-10	MCP-1	RANTES	TNFa
567 ± 32	73 ± 5	3.5 ± 2.8	73 ± 60	956 ± 59	1089 ± 212	9162 ± 170	291 ± 22	10.1 ± 0.3
629 ± 22	85 ± 2	10 ± 4	99 ± 12	1371 ± 13	1209 ± 53	9837 ± 246	686 ± 42 *	10.2 ± 0.5
1.1	1.2	2.9	1.4	1.4	1.1	1.1	2.4	1.0
2955 ± 108	75 ± 7	44 ± 0	136 ± 12	2293 ± 200	2686 ± 153	10754 ± 457	859 ± 5	15.5 ± 0.7
4572 ± 167	115 ± 1	55 ± 2	237 ± 3	3764 ± 93	3969 ± 28 *	13028 ± 965	980 ± 22	16.8 ± 1.4
1.5	1.5	1.3	1.7	1.6	1.5	1.2	1.1	1.1
3167 ± 63	48 ± 3	41 ± 6	128 ± 29	4154 ± 94	1168 ± 22	12360 ± 560	392 ± 23	8.9 ± 0.1
3228 ± 197	75 ± 1	47 ± 0.1	170 ± 10	4436 ± 96	1353 ± 92	15720 ±1086	353 ± 343	9.5 ± 0.7
1.0	1.6	1.1	1.3	1.1	1.2	1.3	0.9	1.1
2979 ± 143	90 ± 8 *	44 ± 1	155 ± 16	3876 ± 213	1834 ± 60 *	13676 ± 1404	396 ± 12	9.1 ± 0.4
0.9	1.9	1.1	1.2	0.9	1.6	1.1	1.0	1.0
1308 ± 49	98 ± 7	21 ± 6	117 ± 10	1874 ± 68	1710 ± 30	10297 ± 58	709 ± 99	13.2 ± 0.3
994 ± 24	92 ± 2	18 ± 7	149 ± 7	2544 ± 77	1869 ± 70	10322 ± 386	666 ± 29	12.6 ± 0.1
0.8	0.9	0.9	1.3	1.4	1.1	1.0	0.9	1.0
338 ± 3	56 ± 1	1.5 ± 0.0	18 ± 1	1228 ± 8	867 ± 72	7226 ± 366	591 ± 341	21.8 ± 1.5
264 ± 12	49 ± 9	5.5 ± 0.0 **	23 ± 4	1529 ± 145	836 ± 73	6240 ± 211	520 ± 40	12.0 ± 0.8
0.8	0.9	3.6	1.3	1.2	1.0	0.9	0.9	0.6
1600 ± 90	50 ± 3	24 ± 0	105 ± 5	1849 ± 38	1262 ± 110	12755 ± 1427	495 ± 7	9.8 ± 0.0
1830 ± 235	48 ± 9	29 ± 7	114 ± 18	1972 ± 103	1099 ± 88	12509 ± 1434	460 ± 138	9.9 ± 1.2
1.1	1.0	1.2	1.1	1.1	0.9	1.0	0.9	1.0
266 ±18	94 ± 16	5.5 ± 0.0	20 ± 2	158 ± 3	12 ± 1	1056 ± 43	1.3 ± 0.4	0.2 ± 0.2
49974 ± 1763 *	138 ± 18	170 ± 6 *	1308 ± 45 *	20734 ± 3283	10465 ± 155 **	13783 ± 1365 *	925 ± 9 **	11068 ± 486 ***
188	1.5	31	65	131	864	13	718	52410

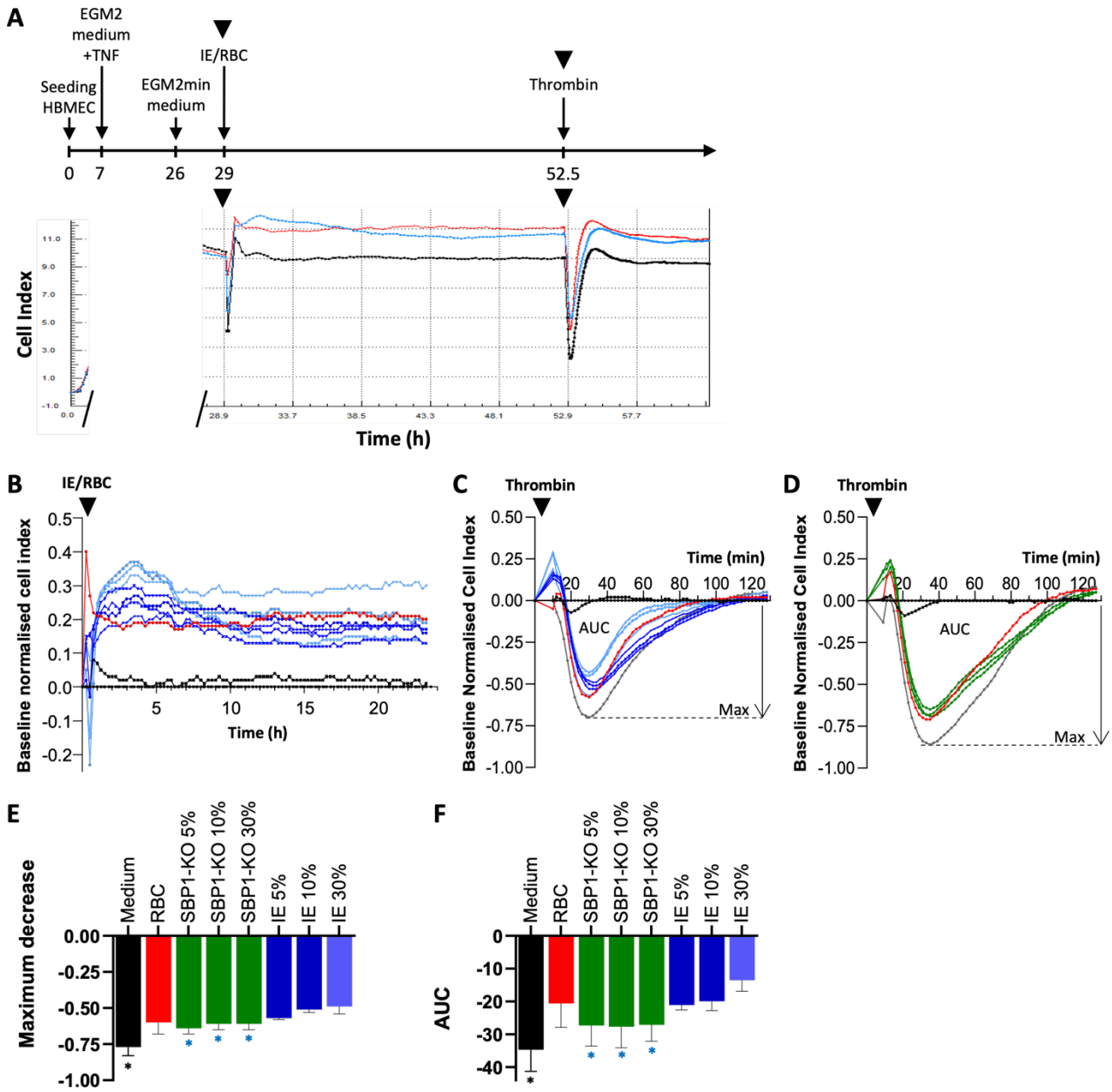

Supplementary Figure 3: **The effect of the patient isolates and SBP1-KO on HBMEC barrier function determined by trans endothelial electrical resistance.** (A) Experimental timeline (not to scale) and a representative cell index trace for IE and thrombin induced changes in HBMEC barrier function. HBMEC were seeded in the E-plate and after approximately 7 hrs the cells were stimulated with 10 ng/ml TNF. The next day, medium was replaced with EGM2min medium and after 2-3 hours, IE at 30% parasitaemia (light blue) or RBC (red), both at 1% HCT, were added. The black line represents medium. After approximately 24 hrs, 5 nM thrombin was added from a concentrated stock solution and cell index was monitored for an additional 10 hours. (B) Cell index trace for the effect of different patient isolates and RBC on HBMEC barrier function of a representative experiment. Cell index was normalised at the time point immediately prior to addition of RBC and IE, indicated by the black triangle, and medium only (black line) was set as baseline. This baseline normalised cell index (BNCI) is shown for 2 UM and 2 CM isolates at 10% parasitaemia (dark blue), 1 UM and 2 CM isolates at 30% parasitaemia (light blue), RBC (red) or replicate medium (black). (C) Thrombin induced decrease in barrier function after 24-hour exposure to patient isolates or RBC. Cell index was normalised at the time point immediately prior to addition of 5 nM thrombin, indicated by the black triangle, and medium without thrombin (black line) was set as baseline. BNCI is shown for medium (dark grey) with the maximum response indicated (max), RBC (red), 1 UM and 2 CM isolates at 30% parasitaemia (light blue) and at 10% parasitaemia (dark blue). (D) As in panel C, but with SBP1-KO at 30% and 10% (green). (E) Maximum decrease of BNCI by thrombin was determined for all co-culture conditions and mean ± SD

are depicted for: control medium (n = 4), RBC (n = 4), SBP1-KO at 5% (n = 3), 10% (n = 3) and 30% parasitaemia (n = 3) and combined patient isolates (IE) at 5% (n = 2), 10% (n = 5) and 30% parasitaemia (n = 5). (F) Area under the curve (AUC) after thrombin induced changes in BNCI was calculated and mean ± SD are depicted for the conditions listed in E. Statistical significance between the various conditions compared to RBC was calculated by unpaired t-test with Welch correction, * p-value < 0.05 (black asterisk). Significance between 30% IE and SBP1-KO was also calculated (blue asterisk).

Supplementary Methods

var Genotyping of Patient Isolates after Culturing

Genotyping of the isolates after culturing was performed by qPCR using selected primers from a *var* gene primer panel as described by Storm et al [26]. RNA was isolated from TRIZOL-stored ring stage IE, DNase treated (TURBO™ DNase, Ambion), cDNA synthesised (Tetro cDNA Synthesis Kit, Bioline) and qPCR carried out with SYBR Green PCR Master Mix (QuantiTect, Qiagen). The endogenous housekeeping genes *seryl-tRNA synthetase* and *aldolase* were used to determine the relative levels of *var* transcripts using the formulae ΔCt *var*-primer = Ct *var* primer minus Ct average of endogenous primers. The transcript unit (Tu) was then calculated as $Tu = 2^{(5-\Delta Ct\ var\text{-}primer)}$. Any low abundance transcripts with a ΔCt *var*-primer >5 was assigned a value of 5, thus subsequently a Tu value of 1. A Tu value of 32 equates to equal transcript levels as the endogenous control genes [65]. The Tu of the patient isolates at the time of isolation from peripheral blood was determined previously [26].

Preparation of HBMEC-IE Co-culture Samples for Phenotypic Analysis

After 6 or 20 hour co-culture with patient isolates, SBP1-KO, RBC or additional controls, co-culture medium was collected, centrifuged for 5 min at 900 g to remove IE, RBC or cellular debris and the supernatant frozen at -80 °C. For cell lysates, HBMEC were washed twice with warm EGM2 medium without supplements and lysed in 50 µl lysis buffer (RIPA buffer (Sigma, R0278) with HALT™ protease inhibitor cocktail (Thermo Scientific, 78429) for 10 minutes on ice. The lysed cells were transferred from the well into a tube, placed on ice for an additional 25 minutes, centrifuged for 5 min at 13,000 g at 4 °C and the supernatant frozen at -80 °C.

Determination of the Concentrations of Prostacyclin and Prostaglandin Endoperoxide Synthase 2

Prostacyclin has a short half-life and therefore its hydrolysis product, 6-keto prostaglandin F1α (6-keto PGF1α), was detected in co-culture medium by competitive ELISA according to the manufacturer's instructions (Cayman Chemicals, 515211). The four UM and four CM isolates and SBP1-KO were co-cultured for 6 hours with their respective RBC as control. The CM4 isolate and SBP1-KO were also co-cultured for 20 hours. As additional controls, HBMEC were incubated with 10 ng/ml TNF for 6 and 20 hours and with 5 nM thrombin for 15 and 30 minutes. Co-culture medium of two independent 6 hour co-

848 culture experiments with the patient isolates, except UM4 and CM2, and SBP1-KO were used, and all
849 samples were measured in duplicate using 2 ELISA plates on the same day. All samples were diluted 2
850 times, but the 20 hour TNF stimulation sample was diluted 5 times. The concentration of 6-keto PGF1α
851 was calculated using the provided standards.
852
853 Prostaglandin endoperoxide synthase 2 (PTGS2) was detected in HBMEC cell lysate by ELISA according
854 to the manufacturer's instructions (Reddot, RD-PTGS2-Hu). Lysates were diluted 5 times and for duplicate
855 samples the concentration of PTGS2 was calculated using the provided standards. On the same day, total
856 protein concentration of the lysates was determined with the BCA kit (Biorad, 5000002) with BSA as
857 standard and ng PTGS2 per mg total protein calculated.
858
859 **Detection of Cytokines and Chemokines**
860 A panel of 41 secreted cytokines and chemokines was measured in the co-culture medium of 6 hours co-
861 culture of HBMEC-IE, HBMEC-RBC and controls using the human cytokine/chemokine 41 plex
862 Immunology Multiplex Assay according to the manufacturer's instructions (Merck, HCYTMAG-60K-
863 PX41). In addition to three CM and two UM isolates, two lab strains, IT4var14 and IT4var37, and a
864 positive control of HBMEC activated by 10 ng/ml TNF for 16 hours were included. The panel included:
865 sCD40L, Eotaxin, FLT-3L, Fractalkine, G-CSF, GM-CSF, GROα, IFNα2, IFNγ, IL-1α, IL-1β, IL-1RA,
866 IL-2, IL-3, IL-4, IL-5, IL-6, IL-7, IL-8, IL-9, IL-10, IL-12 (p40), IL-12 (p70), IL-13, IL-15, IL-17A, IL-
867 17E/IL-25, IL-17F, IL-18, IL-22, IL-27, IP-10, MCP-1, MCP-3, M-CSF, MDC, MIG, MIP-1α, MIP-1β,
868 PDGF-AA, PDGF-AB/BB, RANTES, TGFα, TNFα, TNFβ, VEGF-A.
869
870 **Measuring HBMEC Barrier Integrity**
871 Barrier function was measured by real time Trans Endothelial Electrical Resistance (TEER) analysis with
872 the xCELLigence® RTCA S16 system (ACEA Biosciences). HBMEC cells were seeded at 50,000
873 cells/cm^2 (1x10^4 cells) in Attachment Factor coated E-Plates 16 PET (ACEA Biosciences) in EGM2
874 medium and the arbitrary cell index (CI) was recorded. After approximately 7 hrs the medium was replaced
875 with EGM2 medium with 10 ng/ml TNF and the next day, medium was replaced with EGM2min medium.
876 IE suspensions at 30%, 10% or 5% parasitaemia were prepared at 1% HCT in EGM2min medium and the
877 medium in the E-plate replaced with 100 µl suspension, equivalent to 3x106, 1x106 and 0.5x106 IE,
878 respectively. RBC at 1% HCT and medium only were used as control.
879 After approximately 24 hrs, 5 nM thrombin was added from a concentrated stock solution and cell index
880 was monitored for an additional 10 hours, starting at 2 minute intervals. For analysis, the cell index was
881 normalised either at the time point immediately prior to addition of IE or thrombin (normalised cell index)

882 and medium only was set as baseline (baseline normalised cell index, BNCI). To determine the effect of
883 thrombin, the maximum decrease in BNCI and the area under the curve after recovery to baseline was
884 calculated.
885

886 **References**

887 1 World Malaria Report 2023. Geneva: World Health Organization; 2023. Licence: CC BY-NC-SA 3.0 IGO. (2023).
888 2 Phillips, M. A. *et al.* Malaria. *Nat Rev Dis Primers* **3**, 17050, doi:10.1038/nrdp.2017.50 (2017).
889 3 Kojom Foko, L. P., Kumar, A., Hawadak, J. & Singh, V. Plasmodium cynomolgi in humans: current knowledge and
890 future directions of an emerging zoonotic malaria parasite. *Infection* **51**, 623-640, doi:10.1007/s15010-022-01952-2
891 (2023).
892 4 de Oliveira, T. C. *et al.* Plasmodium simium: Population Genomics Reveals the Origin of a Reverse Zoonosis. *J Infect*
893 *Dis* **224**, 1950-1961, doi:10.1093/infdis/jiab214 (2021).
894 5 Song, X. *et al.* Cerebral malaria induced by plasmodium falciparum: clinical features, pathogenesis, diagnosis, and
895 treatment. *Front Cell Infect Microbiol* **12**, 939532, doi:10.3389/fcimb.2022.939532 (2022).
896 6 Seydel, K. B. *et al.* Brain swelling and death in children with cerebral malaria. *N Engl J Med* **372**, 1126-1137,
897 doi:10.1056/NEJMoa1400116 (2015).
898 7 Mohanty, S. *et al.* Magnetic Resonance Imaging of Cerebral Malaria Patients Reveals Distinct Pathogenetic Processes in
899 Different Parts of the Brain. *mSphere* **2**, doi:10.1128/mSphere.00193-17 (2017).
900 8 Storm, J. & Craig, A. G. Pathogenesis of cerebral malaria--inflammation and cytoadherence. *Front Cell Infect Microbiol*
901 **4**, 100, doi:10.3389/fcimb.2014.00100 (2014).
902 9 Ramachandran, A. & Sharma, A. Dissecting the mechanisms of pathogenesis in cerebral malaria. *PLoS Pathog* **18**,
903 e1010919, doi:10.1371/journal.ppat.1010919 (2022).
904 10 Pasternak, N. D. & Dzikowski, R. PfEMP1: an antigen that plays a key role in the pathogenicity and immune evasion of
905 the malaria parasite Plasmodium falciparum. *Int J Biochem Cell Biol* **41**, 1463-1466, doi:10.1016/j.biocel.2008.12.012
906 (2009).
907 11 Smith, J. D. The role of PfEMP1 adhesion domain classification in Plasmodium falciparum pathogenesis research. *Mol*
908 *Biochem Parasitol* **195**, 82-87, doi:10.1016/j.molbiopara.2014.07.006 (2014).
909 12 Albrecht-Schgoer, K., Lackner, P., Schmutzhard, E. & Baier, G. Cerebral Malaria: Current Clinical and Immunological
910 Aspects. *Front Immunol* **13**, 863568, doi:10.3389/fimmu.2022.863568 (2022).
911 13 Kraemer, S. M. & Smith, J. D. A family affair: var genes, PfEMP1 binding, and malaria disease. *Curr Opin Microbiol* **9**,
912 374-380, doi:10.1016/j.mib.2006.06.006 (2006).
913 14 Bernabeu, M. & Smith, J. D. EPCR and Malaria Severity: The Center of a Perfect Storm. *Trends Parasitol* **33**, 295-308,
914 doi:10.1016/j.pt.2016.11.004 (2017).
915 15 Kessler, A. *et al.* Linking EPCR-Binding PfEMP1 to Brain Swelling in Pediatric Cerebral Malaria. *Cell Host Microbe*
916 **22**, 601-614 e605, doi:10.1016/j.chom.2017.09.009 (2017).
917 16 Turner, L. *et al.* Severe malaria is associated with parasite binding to endothelial protein C receptor. *Nature* **498**, 502-
918 505, doi:10.1038/nature12216 (2013).
919 17 Moxon, C. A., Gibbins, M. P., McGuinness, D., Milner, D. A., Jr. & Marti, M. New Insights into Malaria Pathogenesis.
920 *Annu Rev Pathol* **15**, 315-343, doi:10.1146/annurev-pathmechdis-012419-032640 (2020).
921 18 Lennartz, F. *et al.* Structure-Guided Identification of a Family of Dual Receptor-Binding PfEMP1 that Is Associated with
922 Cerebral Malaria. *Cell Host Microbe* **21**, 403-414, doi:10.1016/j.chom.2017.02.009 (2017).
923 19 Avril, M., Bernabeu, M., Benjamin, M., Brazier, A. J. & Smith, J. D. Interaction between Endothelial Protein C Receptor
924 and Intercellular Adhesion Molecule 1 to Mediate Binding of Plasmodium falciparum-Infected Erythrocytes to
925 Endothelial Cells. *mBio* **7**, doi:10.1128/mBio.00615-16 (2016).
926 20 Gallego-Delgado, J. & Rodriguez, A. Rupture and Release: A Role for Soluble Erythrocyte Content in the Pathology of
927 Cerebral Malaria. *Trends Parasitol* **33**, 832-835, doi:10.1016/j.pt.2017.06.005 (2017).
928 21 Adams, Y. *et al.* Plasmodium falciparum erythrocyte membrane protein 1 variants induce cell swelling and disrupt the
929 blood-brain barrier in cerebral malaria. *J Exp Med* **218**, doi:10.1084/jem.20201266 (2021).
930 22 Bernabeu, M. *et al.* Binding Heterogeneity of Plasmodium falciparum to Engineered 3D Brain Microvessels Is Mediated
931 by EPCR and ICAM-1. *mBio* **10**, doi:10.1128/mBio.00420-19 (2019).
932 23 Zuniga, M. *et al.* Plasmodium falciparum and TNF-alpha Differentially Regulate Inflammatory and Barrier Integrity
933 Pathways in Human Brain Endothelial Cells. *mBio* **13**, e0174622, doi:10.1128/mbio.01746-22 (2022).
934 24 Azasi, Y. *et al.* Infected erythrocytes expressing DC13 PfEMP1 differ from recombinant proteins in EPCR-binding
935 function. *Proc Natl Acad Sci U S A* **115**, 1063-1068, doi:10.1073/pnas.1712879115 (2018).
936 25 Othman, B. *et al.* Different PfEMP1-expressing Plasmodium falciparum variants induce divergent endothelial
937 transcriptional responses during co-culture. *PLoS One* **18**, e0295053, doi:10.1371/journal.pone.0295053 (2023).
938 26 Storm, J. *et al.* Cerebral malaria is associated with differential cytoadherence to brain endothelial cells. *EMBO Mol Med*
939 **11**, doi:10.15252/emmm.201809164 (2019).

27 Maier, A. G. *et al.* Skeleton-binding protein 1 functions at the parasitophorous vacuole membrane to traffic PfEMP1 to the Plasmodium falciparum-infected erythrocyte surface. *Blood* **109**, 1289-1297, doi:10.1182/blood-2006-08-043364 (2007).
28 Livak, K. J. & Schmittgen, T. D. Analysis of relative gene expression data using real-time quantitative PCR and the 2(-Delta Delta C(T)) Method. *Methods* **25**, 402-408, doi:10.1006/meth.2001.1262 (2001).
29 Madkhali, A. M. *et al.* An analysis of the binding characteristics of a panel of recently selected ICAM-1 binding Plasmodium falciparum patient isolates. *PLoS One* **9**, e111518, doi:10.1371/journal.pone.0111518 (2014).
30 Weiss, N., Miller, F., Cazaubon, S. & Couraud, P. O. The blood-brain barrier in brain homeostasis and neurological diseases. *Biochim Biophys Acta* **1788**, 842-857, doi:10.1016/j.bbamem.2008.10.022 (2009).
31 Watson, E. C., Grant, Z. L. & Coultas, L. Endothelial cell apoptosis in angiogenesis and vessel regression. *Cell Mol Life Sci* **74**, 4387-4403, doi:10.1007/s00018-017-2577-y (2017).
32 Vogler, M. BCL2A1: the underdog in the BCL2 family. *Cell Death Differ* **19**, 67-74, doi:10.1038/cdd.2011.158 (2012).
33 Noble, K. E., Wickremasinghe, R. G., DeCornet, C., Panayiotidis, P. & Yong, K. L. Monocytes stimulate expression of the Bcl-2 family member, A1, in endothelial cells and confer protection against apoptosis. *J Immunol* **162**, 1376-1383 (1999).
34 Karsan, A., Yee, E., Kaushansky, K. & Harlan, J. M. Cloning of human Bcl-2 homologue: inflammatory cytokines induce human A1 in cultured endothelial cells. *Blood* **87**, 3089-3096 (1996).
35 Atkins, G. B. & Jain, M. K. Role of Kruppel-like transcription factors in endothelial biology. *Circ Res* **100**, 1686-1695, doi:10.1161/01.RES.0000267856.00713.0a (2007).
36 Sangwung, P. *et al.* KLF2 and KLF4 control endothelial identity and vascular integrity. *JCI Insight* **2**, e91700, doi:10.1172/jci.insight.91700 (2017).
37 Hamik, A. *et al.* Kruppel-like factor 4 regulates endothelial inflammation. *J Biol Chem* **282**, 13769-13779, doi:10.1074/jbc.M700078200 (2007).
38 Ghaleb, A. M. & Yang, V. W. Kruppel-like factor 4 (KLF4): What we currently know. *Gene* **611**, 27-37, doi:10.1016/j.gene.2017.02.025 (2017).
39 SenBanerjee, S. *et al.* KLF2 Is a novel transcriptional regulator of endothelial proinflammatory activation. *J Exp Med* **199**, 1305-1315, doi:10.1084/jem.20031132 (2004).
40 Lin, Z. *et al.* Kruppel-like factor 2 (KLF2) regulates endothelial thrombotic function. *Circ Res* **96**, e48-57, doi:10.1161/01.RES.0000159707.05637.a1 (2005).
41 Stitham, J., Midgett, C., Martin, K. A. & Hwa, J. Prostacyclin: an inflammatory paradox. *Front Pharmacol* **2**, 24, doi:10.3389/fphar.2011.00024 (2011).
42 Ferguson, C. S. & Tyndale, R. F. Cytochrome P450 enzymes in the brain: emerging evidence of biological significance. *Trends Pharmacol Sci* **32**, 708-714, doi:10.1016/j.tips.2011.08.005 (2011).
43 Howard, C., Joof, F., Hu, R., Smith, J. D. & Zheng, Y. Probing cerebral malaria inflammation in 3D human brain microvessels. *Cell Rep* **42**, 113253, doi:10.1016/j.celrep.2023.113253 (2023).
44 Peters, J. M., Fowler, E. V., Krause, D. R., Cheng, Q. & Gatton, M. L. Differential changes in Plasmodium falciparum var transcription during adaptation to culture. *J Infect Dis* **195**, 748-755, doi:10.1086/511436 (2007).
45 Mkumbaye, S. I. *et al.* Cellulose filtration of blood from malaria patients for improving ex vivo growth of Plasmodium falciparum parasites. *Malar J* **16**, 69, doi:10.1186/s12936-017-1714-2 (2017).
46 Cooke, B. M. *et al.* A Maurer's cleft-associated protein is essential for expression of the major malaria virulence antigen on the surface of infected red blood cells. *J Cell Biol* **172**, 899-908, doi:10.1083/jcb.200509122 (2006).
47 Jaffe, E. A., Grulich, J., Weksler, B. B., Hampel, G. & Watanabe, K. Correlation between thrombin-induced prostacyclin production and inositol trisphosphate and cytosolic free calcium levels in cultured human endothelial cells. *J Biol Chem* **262**, 8557-8565 (1987).
48 Werthmann, R. C., Lohse, M. J. & Bunemann, M. Temporally resolved cAMP monitoring in endothelial cells uncovers a thrombin-induced [cAMP] elevation mediated via the Ca(2)+-dependent production of prostacyclin. *J Physiol* **589**, 181-193, doi:10.1113/jphysiol.2010.200121 (2011).
49 Hadjilaou, A., Brandi, J., Riehn, M., Friese, M. A. & Jacobs, T. Pathogenetic mechanisms and treatment targets in cerebral malaria. *Nat Rev Neurol* **19**, 688-709, doi:10.1038/s41582-023-00881-4 (2023).
50 Moxon, C. A. *et al.* Parasite histones are toxic to brain endothelium and link blood barrier breakdown and thrombosis in cerebral malaria. *Blood Adv* **4**, 2851-2864, doi:10.1182/bloodadvances.2019001258 (2020).
51 Avril, M., Benjamin, M., Dols, M. M. & Smith, J. D. Interplay of Plasmodium falciparum and thrombin in brain endothelial barrier disruption. *Sci Rep* **9**, 13142, doi:10.1038/s41598-019-49530-1 (2019).
52 Moxon, C. A. *et al.* Loss of endothelial protein C receptors links coagulation and inflammation to parasite sequestration in cerebral malaria in African children. *Blood* **122**, 842-851, doi:10.1182/blood-2013-03-490219 (2013).
53 Bachmann, A. *et al.* Highly co-ordinated var gene expression and switching in clinical Plasmodium falciparum isolates from non-immune malaria patients. *Cell Microbiol* **13**, 1397-1409, doi:10.1111/j.1462-5822.2011.01629.x (2011).
54 Lee, W. C., Russell, B. & Renia, L. Sticking for a Cause: The Falciparum Malaria Parasites Cytoadherence Paradigm. *Front Immunol* **10**, 1444, doi:10.3389/fimmu.2019.01444 (2019).
55 Chan, J. A. *et al.* A single point in protein trafficking by Plasmodium falciparum determines the expression of major antigens on the surface of infected erythrocytes targeted by human antibodies. *Cell Mol Life Sci* **73**, 4141-4158, doi:10.1007/s00018-016-2267-1 (2016).

1002 56 Possemiers, H. *et al.* Skeleton binding protein-1-mediated parasite sequestration inhibits spontaneous resolution of
1003 malaria-associated acute respiratory distress syndrome. *PLoS Pathog* **17**, e1010114, doi:10.1371/journal.ppat.1010114
1004 (2021).
1005 57 Pino, P. *et al.* Plasmodium falciparum--infected erythrocyte adhesion induces caspase activation and apoptosis in human
1006 endothelial cells. *J Infect Dis* **187**, 1283-1290, doi:10.1086/373992 (2003).
1007 58 Dorris, S. L. & Peebles, R. S., Jr. PGI2 as a regulator of inflammatory diseases. *Mediators Inflamm* **2012**, 926968,
1008 doi:10.1155/2012/926968 (2012).
1009 59 Xu, S. *et al.* The zinc finger transcription factor, KLF2, protects against COVID-19 associated endothelial dysfunction.
1010 *Signal Transduct Target Ther* **6**, 266, doi:10.1038/s41392-021-00690-5 (2021).
1011 60 Zhou, G. *et al.* Endothelial Kruppel-like factor 4 protects against atherothrombosis in mice. *J Clin Invest* **122**, 4727-4731,
1012 doi:10.1172/JCI66056 (2012).
1013 61 O'Carroll, S. J. *et al.* Pro-inflammatory TNFalpha and IL-1beta differentially regulate the inflammatory phenotype of
1014 brain microvascular endothelial cells. *J Neuroinflammation* **12**, 131, doi:10.1186/s12974-015-0346-0 (2015).
1015 62 Storm, J., Wu, Y., Davies, J., Moxon, C. A. & Craig, A. G. Testing the effect of PAR1 inhibitors on Plasmodium
1016 falciparum-induced loss of endothelial cell barrier function. *Wellcome Open Res* **5**, 34,
1017 doi:10.12688/wellcomeopenres.15602.3 (2020).
1018 63 Alberelli, M. A. & De Candia, E. Functional role of protease activated receptors in vascular biology. *Vascul Pharmacol*
1019 **62**, 72-81, doi:10.1016/j.vph.2014.06.001 (2014).
1020 64 Moxon, C. A. *et al.* Persistent endothelial activation and inflammation after Plasmodium falciparum Infection in
1021 Malawian children. *J Infect Dis* **209**, 610-615, doi:10.1093/infdis/jit419 (2014).
1022 65 Mkumbaye, S. I. *et al.* The Severity of Plasmodium falciparum Infection Is Associated with Transcript Levels of var
1023 Genes Encoding Endothelial Protein C Receptor-Binding P. falciparum Erythrocyte Membrane Protein 1. *Infect Immun*
1024 **85**, doi:10.1128/IAI.00841-16 (2017).
1025